Synthesis and Characterization of MOG-IDAC and PLP-PEG-B7AP Molecules for Efficacy Evaluation in the EAE mouse model

By

2012

John M. Stewart

Submitted to the Department of Pharmaceutical Chemistry and the Graduate Faculty of the University of Kansas in partial fulfillment of the requirements for the degree of Master of Science.

_____

Chairperson Teruna J. Siahaan

_____

Cory J. Berkland

_____

Thomas Tolbert

Date Defended: December 12, 2012

The Thesis Committee for John M. Stewart

certifies that this is the approved version of the following thesis:

Synthesis and Characterization of MOG-IDAC and PLP-PEG-B7AP Molecules for Efficacy Evaluation in the EAE mouse model

_____

Chairperson Teruna J. Siahaan

Date approved: 3/12/2013

Synthesis and Characterization of MOG-IDAC and PLP-PEG-B7AP Molecules for Efficacy Evaluation in the EAE mouse model

John Stewart

The University of Kansas, 2012

Synthesis, Formulation, and In vivo Evaluation of MOG-PEG-IDAC and PLP-PEG-B7AP for Targeting APC to Suppress EAE

John M. Stewart, Crisandra Wilkie, Barlas Buyuktimkin, Ahmed Badawi, Paul Kiptoo, and Teruna J. Siahaan

Department of Pharmaceutical Chemistry, The University of Kansas, Lawrence KS, 66047

There are two long-term objective of this project **1.** Is to use a novel I-Domain Antigen Conjugate (IDAC) molecule to target antigenic peptide to APC to control autoimmune diseases. The short-term objectives of this project are to synthesize, formulate, and evaluate the efficacy of Myelin Oligodendrocyte Glycoprotein (MOG) MOG-PEG-IDAC molecules in suppressing Experimental Autoimmune Encephalomyelitis (EAE) in animal models. The MOG-PEG-IDAC molecule is hypothesized to simultaneously bind to major histocompatibility complex II (MHC-II) and intercellular adhesion molecule 1 (ICAM-1) on the surface of antigen-presenting cells (APC). **2.** Is to evaluate the efficacy of PLP-PEG-B7AP in suppressing EAE in mice. The PLP-PEG-B7AP molecule is hypothesized to simultaneously bind to the MHC-II and B7 molecule on the surface of the APC. This binding blocks the formation of the "immunological synapse" and will generate the regulatory response to suppress EAE. Two specific aims are proposed to carry out the short-term objectives. The first specific aim is to design MOG-PEG-IDAC molecules. The second specific aim is to evaluate the efficacy of PLP-PEG-B7AP in suppressing EAE in animal models. To date, the synthesis and characterization of the MOG-PEG-IDAC has been completed, along with EAE animal studies of the PLP-PEG-B7AP.

Acknowledgments

I first would like to thank my mentor Dr. Teruna J. Siahaan for helping me apply for graduate studies here at the University of Kanas. I also would like to thank him for his tutelage in course work, lab, and life. He has truly helped me to grow during my time as a student in his lab.

I would also like to thank my committee members Dr. Teruna J. Siahaan, Dr. Cory Berkland, and Dr. Thomas Tolbert. They all have provided me with feedback on my progress in my research for this thesis and given me valuable advice on how to accomplish my intended goals.

I owe a great deal of gratitude to my mother Debra A. Foster, my sister Danielle M. Stewart, brother David A. Stewart and my father John M. Stewart Sr. for providing me with the encouragement when I felt down.

I also have much gratitude for my past and current peers and fellow friends in lab: Dr. Paul Kiptoo, Dr. Ahmed Badawi, Dr. Barlas Büyüktimkin, Dr. Prakash Manikwar, Dr. Vivit Dewtri, Marlyn Lakistorini, Ahmed Alaofi, Mohammed Al-Saman, Kayann Tabanor, Crissandra Wilkie, and Matt Behymer. All of these people have provided much needed help and information in accomplishing my goals.

I would also like to thank my fellow peers in my graduate program. They have to provided me with invaluable advice and are all considered my friends, and have made my life here in Lawrence very enjoyable!

I would like to specially thank Dr. Barlas Büyüktimkin, Dr. Ahmed Badawi, and Dr. Paul Kiptoo. They were instrumental in providing me with the necessary training and knowledge to complete my research in this thesis.

Table of Contents

Chapter 1

Synthesis, Formulation, and In vivo Evaluation of MOG-PEG-IDAC and PLP-PEG-B7AP for Targeting APC to Suppress EAE

The long-term goal of this project is to develop therapeutic molecules to treat autoimmune diseases such as multiple sclerosis (MS), type-1 diabetes, and rheumatoid arthritis in an antigen-specific manner without suppressing the general immune response. The short-term goals of this project are to synthesize I-domain antigenic-peptide conjugate (IDAC) molecules and bifunctional peptide inhibitor (BPI) molecules with MOG and PLP peptides and evaluate their in vivo efficacy to suppress EAE in the animal model. To accomplish our short-term goals, we carried out two different Specific Aims:

Specific Aim 1: To synthesize and characterize MOG-IDAC and MOG-PEG-IDAC for their efficacy evaluation in MOG-stimulated EAE in mice. This work is described in Chapter 2.

Specific Aim 2: To synthesize PLP-PEG-B7AP molecule and evaluate its efficacy as a "therapeutic vaccine" in the EAE animal model. This work is described in Chapter 3.

MS is a neurological autoimmune disease in which the activated T-cells recognize self-proteins of the myelin sheath as antigens. As a result, an inflammatory response is initiated within the central nervous system (CNS) to demyelinate the axons of nerve cells. Experimental autoimmune encephalomyelitis (EAE) is an animal model that has been used to evaluate therapeutic agents for treating MS. This animal model has disease characteristics similar to those of MS. For example, antigenic proteins such as myelin basic protein (MBP), proteolipid protein (PLP), and myelin oligodendrocyte glycoprotein (MOG) that elicit the autoimmune response are similar in both MS and EAE. Current therapies for MS that focus on suppressing the general immune response lack specificity and leave the patient susceptible to infection. The objective of this project is to develop conjugates of antigenic peptides that target the antigen-presenting cells (APC) for modulating subpopulations of T cells from inflammatory phenotype to

regulatory/suppressor phenotype. To accomplish this objective, our group synthesized and evaluated the efficacy of bi-functional peptide inhibitors (BPI) and I-domain antigenic-peptide conjugates (IDAC). These molecules are designed to simultaneously target the major histocompatibility complex II (MHC II) and adhesion receptors on APC to inhibit the immunological synapse formation and prevent the activation of T cells.

Our previous data showed that PLP-IDAC can significantly suppress PLP-induced EAE in mice when administered in prophylactic and vaccine-like manners. PLP-IDAC decreases the production of inflammatory cytokines (*e.g.*, IL-17) and increases the production of regulatory cytokines (*e.g.*, IL-10), suggesting a shift in T-cell proliferation from an inflammatory to a regulatory phenotype. An IDAC molecule contains multiple antigenic peptides ranging from 4 to 8; this property provides a unique opportunity for simultaneously delivering multiple antigenic peptides from PLP, MOG, and MBP to prevent antigenic spreading in MS. However, in carrying out the evaluation of a multiantigen IDAC molecule, we have to demonstrate that an IDAC molecule with another antigen such as MOG or MBP peptides (i.e., MOG-IDAC or MBP-IDAC) could also suppress EAE effectively. In this study, MOG peptide (*i.e.*, MOG-Cys) was conjugated to the I-domain to make MOG-IDAC and MOG-PEG-IDAC. The synthesis of MOG-IDAC was inefficient, and the amount of product could only be used for chemical and physical characterization; there was not a sufficient amount to carry out animal studies. This inefficiency was due to the insolubility of the MOG-Cys peptide. Therefore, MOG-Cys peptide was modified to MOG-PEG-Cys peptide with polyethylene glycol groups in between the MOG peptide sequence and the Cys residue. Conjugation of MOG-PEG-Cys and the I-domain successfully produced MOG-PEG-IDAC. The purpose of the second chapter is to describe the synthesis and

characterization of MOG-IDAC and MOG-PEG-IDAC molecules. The efficacy study of this MOG-PEG-IDAC is still ongoing.

In our earlier work, a novel PLP-B7AP molecule was found to effectively suppress PLP-stimulated EAE in mice upon administration of the peptide as a prophylactic; different from PLP-BPI with LABL peptide, this molecule contains another costimulatory peptide derived from the CD28 sequence that binds to B7 receptors. However, the PLP-B7AP molecule has not been evaluated in vaccine-like treatment of EAE in the mouse model. In the third chapter, we designed PLP-PEG-B7AP to improve solubility and evaluate its efficacy as a vaccine-like treatment to suppress EAE. PLP-PEG-B7AP has a polyethylene glycol group as a linker. MOG-PEG-B7AP was also synthesized, and the efficacy of MOG-PEG-B7AP is being investigated in MOG-stimulated EAE.

Chapter 2

Synthesis and Characterization of MOG-IDAC and MOG-PEG-IDAC

2.1. Introduction

The damage in myelin sheaths around the nerve axons is one of the pathogenesis of multiple sclerosis (MS) where nerve signal transmission is slowed down or completely disrupted [1]. Therefore, MS is characterized as neurological autoimmune disease that is signified by inflammation and demyelination of the central nervous system (CNS) due to the presence of autoreactive T-cells in the CNS [2]. The permanent loss of protective myelin sheath of the nerve axons leads to irreversible neurological dysfunction in chronic MS patients [1]. Up to now, the triggers that cause MS in patients have not been elucidated; however, several different pathogeneses of the disease have been proposed, including patient's multiple exposure to Epstein-Barr virus infections, environmental factors, stressful life events, and genetic inheritance [3-7]. Much like other autoimmune diseases (e.g., rheumatoid arthritis (RA) and type-1 diabetes), MS pathogenesis involves autoreactive T and B cells that are stimulated during inflammatory immune response to produce the disease onset and progression [8, 9].

There are several therapeutic agents currently used to treat MS as well as in clinical trials, including Fingolimod (FTY720), Natalizumab (Tysabri®), IFNB-1b (Betaseron®), Mitoxantrone (Novantrone®), and glatiramer acetate (COP1, Copaxone®) [10-15]. These treatments have varying mechanisms of action but they operate on the premise of suppressing general immune responses instead of preventing and stopping the cause of MS. Therefore, there is a need to develop novel therapeutic agents that target and suppress a specific sub-population of immune cells that are involved in generating the disease without suppressing the general immune responses.

To find a new way to treat MS, our group has recently developed a novel way to suppress the activation of a selected sub-population of immune cells such as inflammatory T cells (*i.e.*, Th-17

and Th-1) and to induce the proliferation of regulatory T cells (T-reg). This new method uses bi-functional peptide inhibitor (BPI) molecules that consist of a cell adhesion peptide linked to an antigenic peptide to target the antigenic peptide to antigen-presenting cells (APC) for altering the differentiation and proliferation of naïve T cells to regulatory/suppressor T cells (T-reg and Th2) for suppressing the disease [16].

Our previous studies have shown that BPI molecules suppressed autoimmune diseases in animal models for rheumatoid arthritis, type-1 diabetes (T1D) [17] and MS [2, 8, 18-22]. BPI molecules have been shown to effectively suppress experimental autoimmune encephalomyelitis (EAE) in the mouse model. In this case, BPI molecules were designed by conjugating antigenic peptides from myelin sheath proteins such as proteolipid protein (PLP), myelin oligodendrocyte protein (MOG), and myelin basic protein (MBP). Although Myelin sheath proteins are considered autoantigens recognized by T cells in the development of MS [23], injections of soluble form of peptides from the epitopes of these "autoantigens" can suppress EAE in mice [2, 24]. Interestingly, BPI molecules are more effective than autoantigen peptide alone. The proposed mechanism of action of BPI molecules is that they bind simultaneously to the major histocompatibility complex class II (MHC-II) and ICAM-1 on the APC and block the immunological synapse formation at the APC-T-cell interface. This event causes a shift of T-cell differentiation from inflammatory to regulatory phenotypes [2, 17, 20, 21]. The study has now been extended to evaluate the efficacy of MOG-BPI, which is a conjugate between $MOG_{(38-50)}$ and LABL ($CD11a_{237-246}$) peptides; MOG-BPI has been shown to be more effective than $MOG_{(38-50)}$ peptide in suppressing of MOG-induced EAE in the mouse model [18].

Previously, multiple $PLP_{(139-151)}$ peptides were conjugated to the lysine residues of the I-domain of LFA-1 protein to make I-domain antigen conjugates (IDAC) molecules (i.e., PLP-

IDAC) and PLP-IDAC can effectively suppress EAE in the animal model presumably by blocking both signal-1 and signal-2 of the immunological synapse [25, 26]. IDAC molecules have an advantage of delivering multiple antigens due to multiple conjugations of antigen to the I-domain protein[25]. In this study, we explored the possibility of conjugating several $MOG_{(38-50)}$ peptides to the I-domain to make MOG-IDAC or MOG-PEG-IDAC molecules for potential evaluation of their efficacies in MOG-stimulated EAE. Thus, the MOG-IDAC and MOG-PEG-IDAC were synthesized by conjugating the multiple MOG-Cys and MOG-PEG-Cys to gamma-maleimido-butyramide (GMB) groups on the lysine residues of the I-domain protein. The resulting MOG-IDAC or MOG-PEG-IDAC was purified using size exclusion chromatography and characterized using SDS-PAGE, mass spectrometry and circular dichroism (CD) spectroscopy.

2.2 Experimental Procedures

2.2.1. Materials. Amino acids used in peptide synthesis were purchased from Peptide International Inc. (Louisville, KY). GMBS (N-[γ-maleimidobutryloxy]succinimide ester) was purchased from Pierce Inc. (Rockford, IL). All other chemicals and solvents used were of analytical grade.

2.2.2 Peptide Synthesis. The MOG-Cys (Ac-GWYRSPFSRVVHLC-NH_2) and MOG-PEG-Cys (Ac-GWYRSPFSRVVHL-Peg-Peg-C-NH_2) peptides were synthesized with automated peptide synthesizer (Pioneer; Perceptive Biosystems, Framingham, MA) using Fmoc chemistry as previously described (see reference [2]). A list of peptides used can be found in table 2.1.

After peptide cleavage from the resin using trifluoroacetic acid (TFA), the crude peptides were purified by reversed-phase high performance liquid chromatography (HPLC) on a semi-preparative C18 column with a gradient of solvent A (94.9% H_2O, 5% Acetonitrile, 0.1% TFA) and solvent B (100% acetonitrile). Analytical HPLC was used to determine the purity of each peptide fraction collected from a semi-preparative HPLC. Fractions that showed high purity were then pooled together and lyophilized. ESI mass spectrometry indicated that the pure MOG-Cys (M+H = 1748.075) and MOG-PEG-Cys (M+H = 2126.39) have the correct molecular weights.

Peptide	**Sequence**	**Molecular Weight**
MOG-Cys	Ac-GWYRSPFSRVVHLC-NH2	1748.075
MOG-PEG-Cys	Ac-GWYRSPFSRVVHL-PEG-PEG-C-NH2	2126.39

Table 2.1. Peptides used in current study. Peptides sequences of both MOG-Cys and MOG-PEG-cys peptides.

2.2.3 Preparation of the I-domain. The I-domain protein was previously overexpressed, refolded, and purified using methods described in earlier work [27]. The purity and structural properties of the I-domain protein were evaluated by mass spectrometry, SDS-PAGE, and CD.

2.2.4. Synthesis of MOG-IDAC and MOG-PEG-IDAC. The MOG-IDAC and MOG-PEG-IDAC were synthesized via the formation GMB-I-domain, which was synthesized by reacting several lysine residues with N-[γ-maleimidobutyryloxy]-succinimide ester (GMBS)

(Figure 2.1). In this case, the I-domain protein (20 mg) was dissolved in 10 ml of buffer (2 mg/ml) followed by drop-wise addition of 10 fold molar excess of GMBS in 500 µl of DMSO. The mixture was stirred for 1 h at 24°C in the absence of light and the crude GMB-I-domain was purified using a Superdex 75 size exclusion chromatography (SEC) column in PBS containing 10 mM $MgSO_4$. After combining all SEC fractions containing GMB-I-domain, the solution was concentrated using ultrafiltration. The number of GMB group per I-domain molecules was determined by MALDI-TOF mass spectrometry.

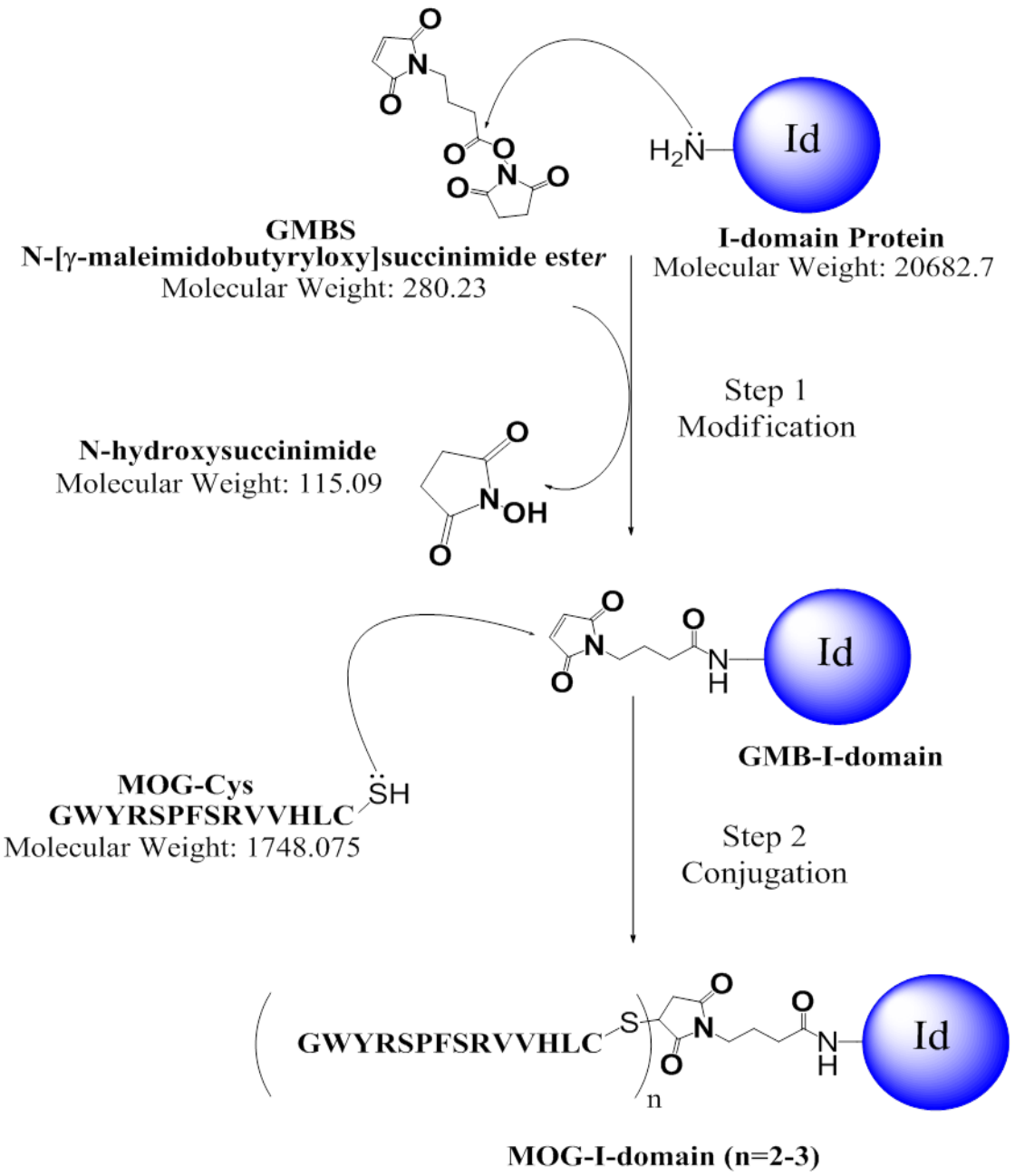

Figure 2.1. The reaction steps to make MOG-IDAC or MOG-PEG-IDAC. The first step is to derivatize the lysine residues on the I-domain to gamma-maleimido-butyramide (GMB) groups. Then in step 2, the maleimide groups are reacted with the thiol group of the cysteine residue on the MOG peptide to produce the desired conjugates.

To complete the synthesis of MOG-IDAC or MOG-PEG-IDAC, the maleimide groups on the GMB-I-domain were reacted with the thiol group of MOG-Cys or MOG-PEG-Cys. In this reaction, 15 fold molar excess of the peptide (MOG-Cys or MOG-PEG-Cys) was added drop-wise into a solution of GMB-I-domain (2.0 mg/ml) at pH 7.5; then, the reaction was carried out for 1 hour at 24°C with constant stirring under dark conditions. The resulting MOG-IDAC or MOG-PEG-IDAC was purified on a Superdex 75 size exclusion column and eluted with PBS containing 10 mM $MgSO_4$. The fractions containing the MOG-IDAC or MOG-PEG-IDAC were collected and concentrated by ultrafiltration and the number of peptides conjugated to the I-domain was determined by MALDI-TOF mass spectrometry. The purity of the IDAC molecules was confirmed by SDS-PAGE gel and size-exclusion chromatography. The secondary structure was confirmed by far-UV CD and compared to the parent GMB-I-domain and I-domain.

2.2.5. Gel Electrophoresis. The purity of protein solution of I-domain, GMB-I-domain, MOG-IDAC, MOG-PEG-IDAC obtained from SEC separation was analyzed by SDS-PAGE. Approximately 100 μg of protein in solution was mixed with 4x Tris-glycine SDS sample buffer without reducing agent and loaded into 1.5 mm thick 10 well NuPAGE Novex 4–12% Bis-Tris gradient gel. The gel was run for 1 h at 150 V, then was stained with 0.25% coomassie blue R250 solution (10% acetic acid, 50% ethanol, 40% water) for 30 min followed by destaining (10% acetic acid, 25% ethanol, 65% water) until the bands were visible and the background was completely clear.

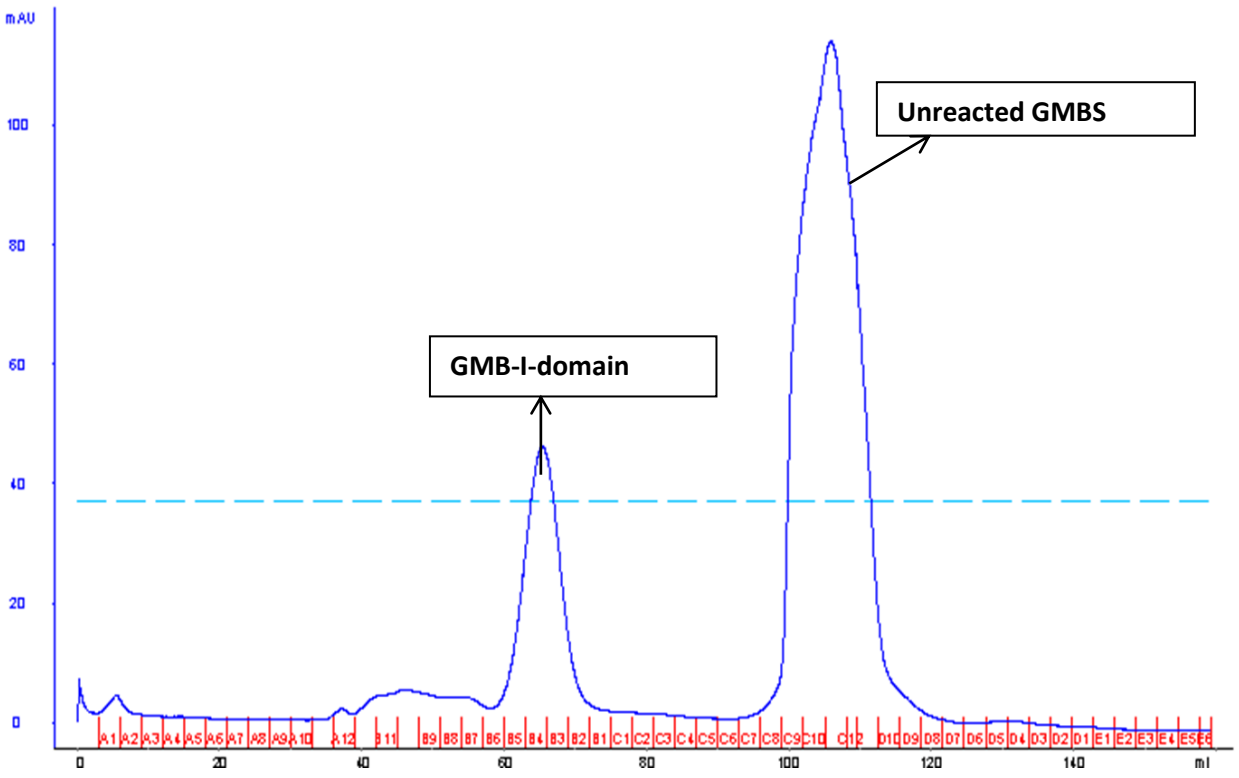

Figure 2.2. SEC Chromatogram of GMB-I-Domain. SEC chromatogram showing the separation between GMB-I-domain and unreacted GMBS. The crude reaction of reaction between GMBS and I-domain was purified using Superdex 75 column eluted with PBS with 10 mM $MgSO_4$.

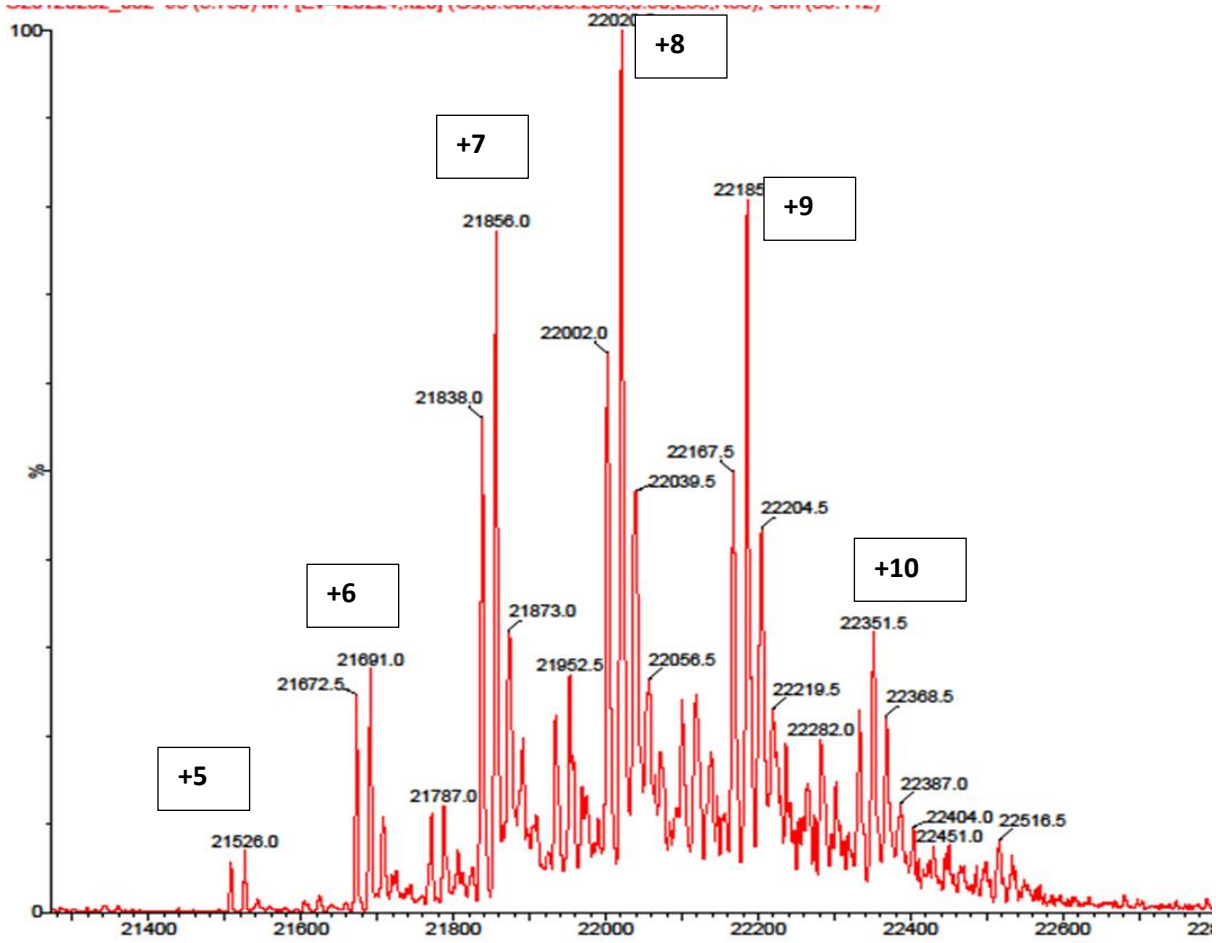

Figure 2.3. MALDI-TOF mass spectrum of GMB-I-domain protein. The conjugates contain 5 to 10 GMB groups per I-domain molecule.

2.3. Results

2.3.1. Conjugation of GMBS to I-domain. The formation of GMB-I-domain was very efficient and it can readily be separated from the unreacted GMBS using SEC (Figure 2.2). The pure GMB-I-domain has 5 to 10 GMB groups attached per I-domain molecule as determined by MALDI-TOF mass spectrometry (Figure 2.3). The parent I-domain with a molecular weight of 20,682 Da (previous data) [25] was not observed in the MS spectra of the GMB-I-domain conjugates. The mass spectrometry demonstrated multiple conjugates of GMB to I-domain protein with molecular weights of 21,526 Da, 21,691 Da, 21,856 Da, 22,020 Da, 22,185 Da, 22,351 Da with a difference of 165 Da for a GMB group (Figure 2.3). The first peak with 21,526 Da was from GMB-I-domain with 5 GMB groups; thus, the remaining peaks correspond to GMB-I-domain with 6 to 10 GMB groups, respectively. The mass spectrum of GMB-I-domain also produced peaks with corresponding peaks of 18 Da mass increased (Figure 2.3), which were due to the hydrolysis of the attached maleimide groups. These results are consistent with the SDS PAGE gel that indicates two bands of the desired maleimide conjugate and maleic acid derivatives, which have different electrophoretic mobility (Figure 2.4, lane 3). In the case of the parent I-domain, only one band appears on the gel (Figure 2.4, lane 2). The formation of hydrolysis products from the GMB-I-domain increases upon storage, so it is necessary that the GMB-I-domain be used for the next conjugation reaction within 48 hours of SEC purification. In order to better understand the structure of the GMB-I-domain conjugate the secondary structure of GMB-I-domain was compared to the I-domain using CD spectroscopy (Figure 2.5) and both molecules have similar secondary structure.

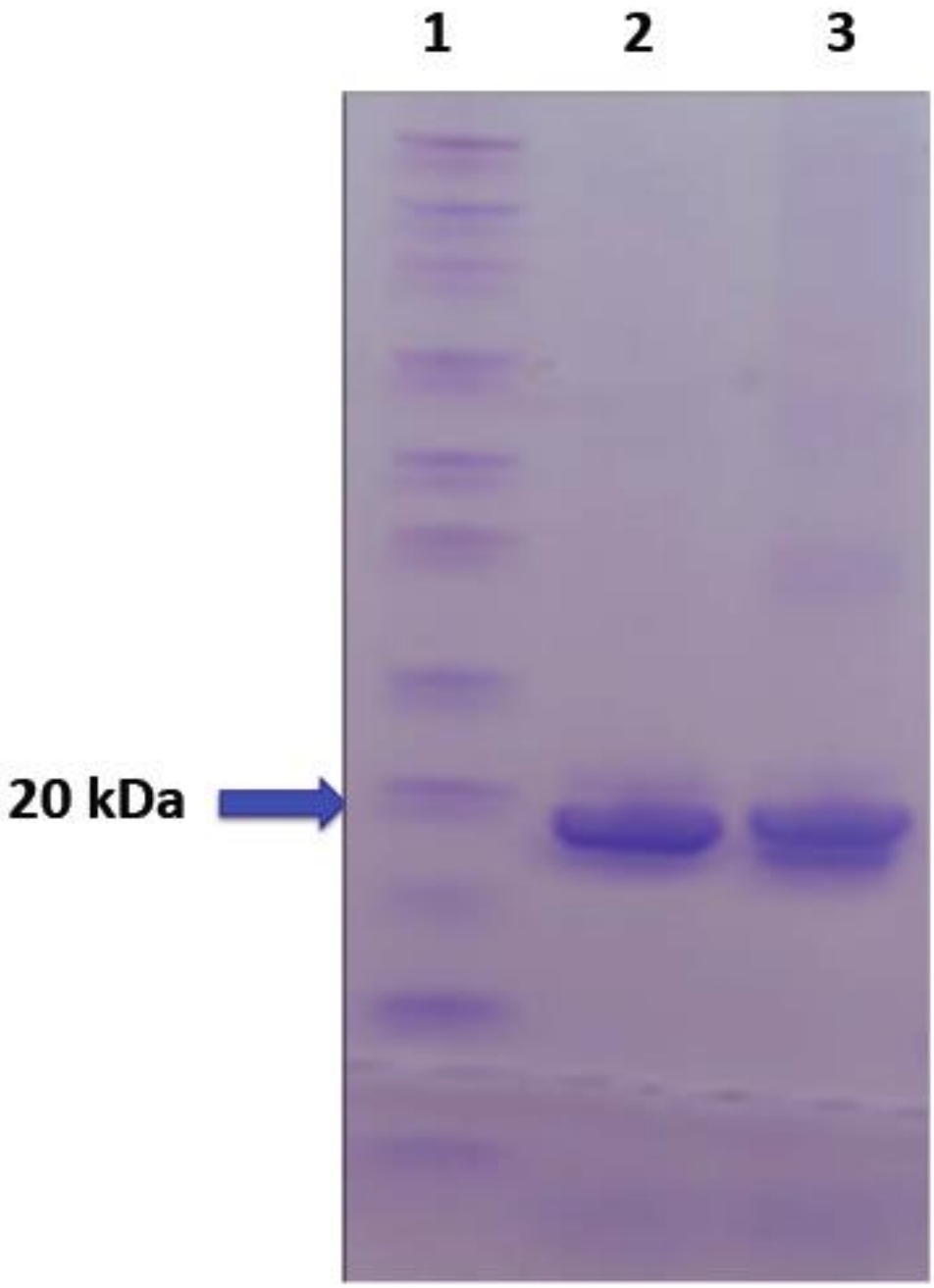

Figure 2.4. SDS-PAGE of GMB-I-Domain. SDS-PAGE analysis of pure GMB-I-domain compared to the I-domain protein after SEC purification. The gel was stained with staining coomassie blue: lane 1 for marker molecules, lane 2, for I-domain, and lane 3 for GMB-I-domain.

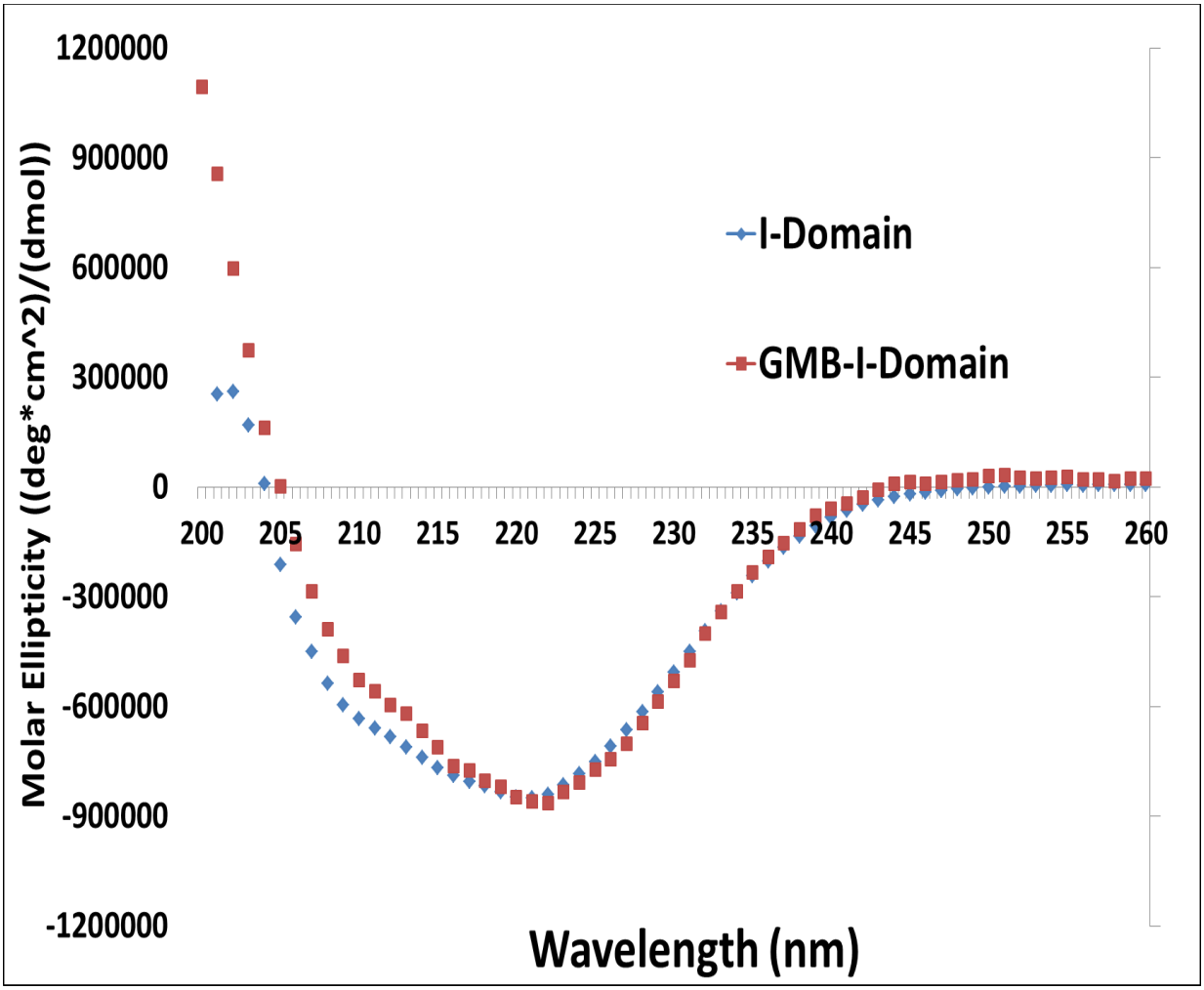

Figure 2.5. CD Spectra of GMB-I-Domain. GMB-I-domain (Blue) has similar CD spectrum with the parent I-domain (Red).

2.3.2. Synthesis of MOG-IDAC. MOG-IDAC was synthesized by conjugating MOG-Cys to the GMB-I-domain at pH 7.5 using previously described method [25]. MOG-Cys is the $MOG_{(38-50)}$ peptide with an additional cysteine amino acid at the C-terminus and the peptide was also amidated and acetylated at the N- and C-terminus. The peptide conjugation is via nucleophilic attack on the maleimide groups of the GMB-I-domain by the thiol group of the Cys residue on MOG-Cys (Step 2, Figure 2.1). The crude sample of the MOG-IDAC was analyzed by SDS-PAGE against the parent I-domain and GMB-I-domain (Figure 2.6). The gel of the crude product of MOG-IDAC (lane 6, Figure 2.6) shows multiple bands at around 20 kDa, indicating the protein is a mixture of conjugates different amount of conjugated peptides. Lane 6 also illustrates the presence of a lower MW bands corresponding to excess MOG-Cys peptide. The parent I-domain (lane 2) shows one single band with lower molecular weight than GMB-I-domain (lane 4) and MOG-IDAC (lane 6).

The reaction mixture was purified through SEC and the eluted fractions of desired pure MOG-IDAC were pooled and concentrated. Unlike the SDS-PAGE of the crude product, the pure fraction shows a single peak at the desired product without the presence of MOG-Cys peptide peak (Figure 2.7). The pure product was subjected to MALDI-TOF MS analysis and multiple peaks were observed to indicate 1 to 2 of MOG-Cys peptides conjugated to a molecule of I-domain (Figure 2.8). Finally, the CD spectrum of MOG-IDAC was compared to GMB-I-domain and parent I-domain (Figure 2.9) and the results confirm that MOG-IDAC has similar secondary structure with GMB-I-domain and I-domain.

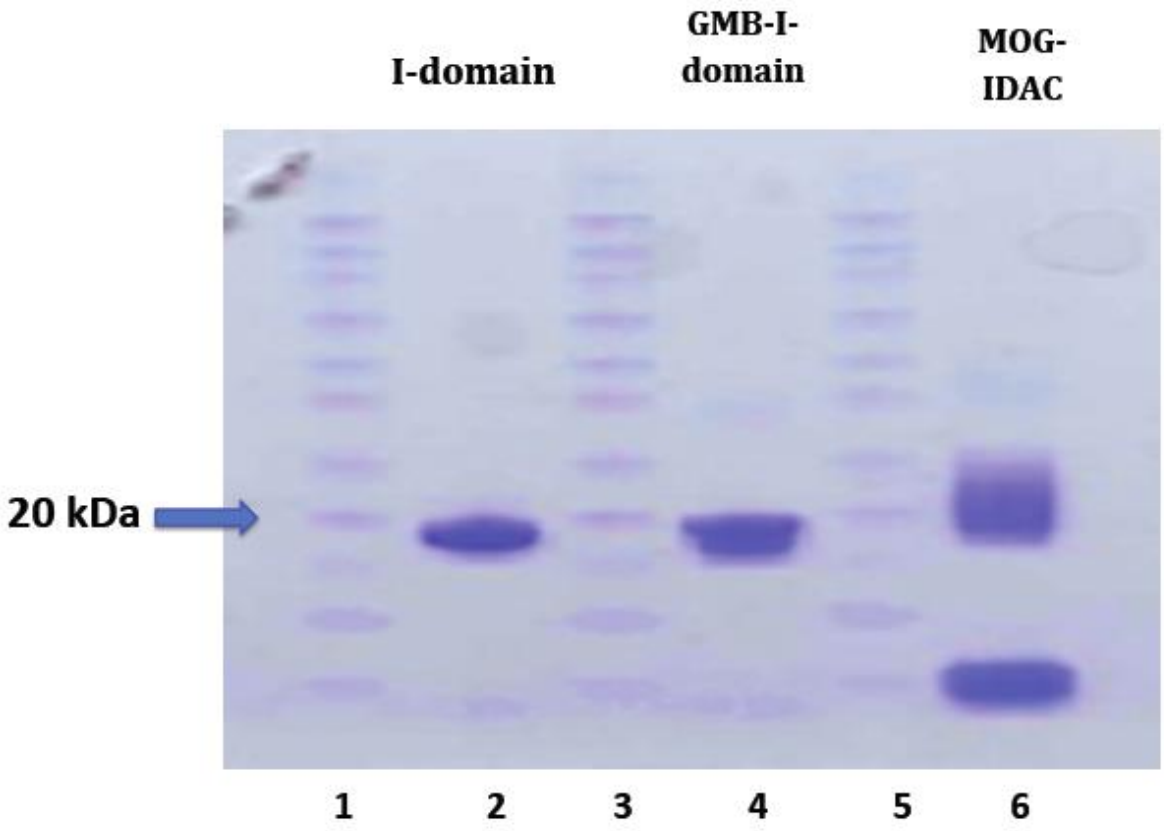

Figure 2.6. The SDS-PAGE of the crude reaction to make MOG-IDAC. Compared to GMB-I-domain (lane 4) and I-domain (lane 2). In lane 6, the MOG-IDAC shows multiple products around 20 kDa with different number of conjugated peptides. The crude also shows peptide band at a low molecular weight.

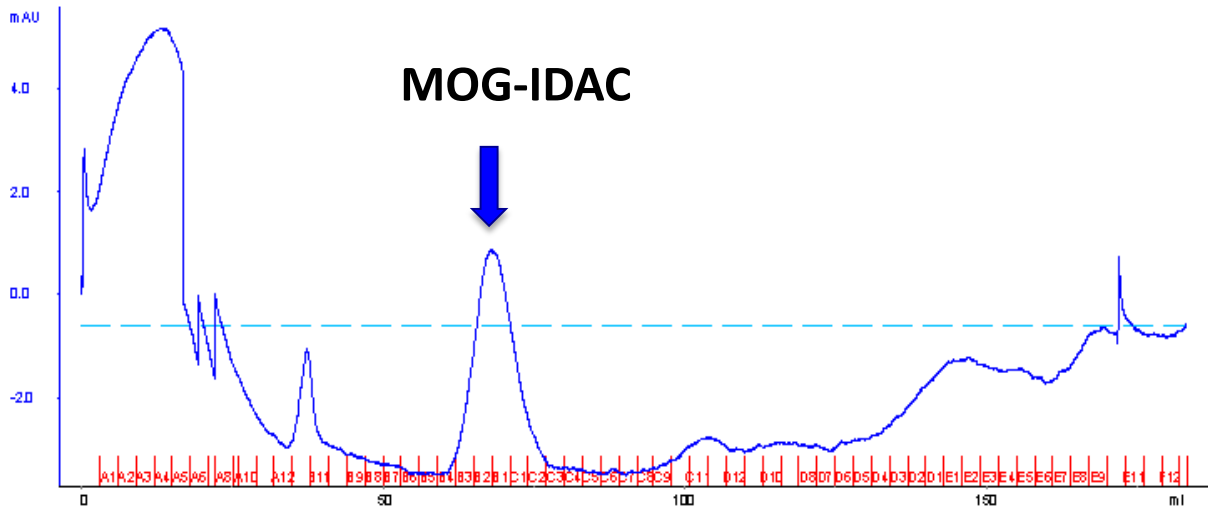

Figure 2.7. SEC Chromatogram of MOG-IDAC. Analytical SEC chromatogram of MOG-IDAC after purification using Superdex 75 column eluted with PBS with 10 mM $MgSO_4$. The chromatogram did not show any peak for the left over MOG-Cys peptide.

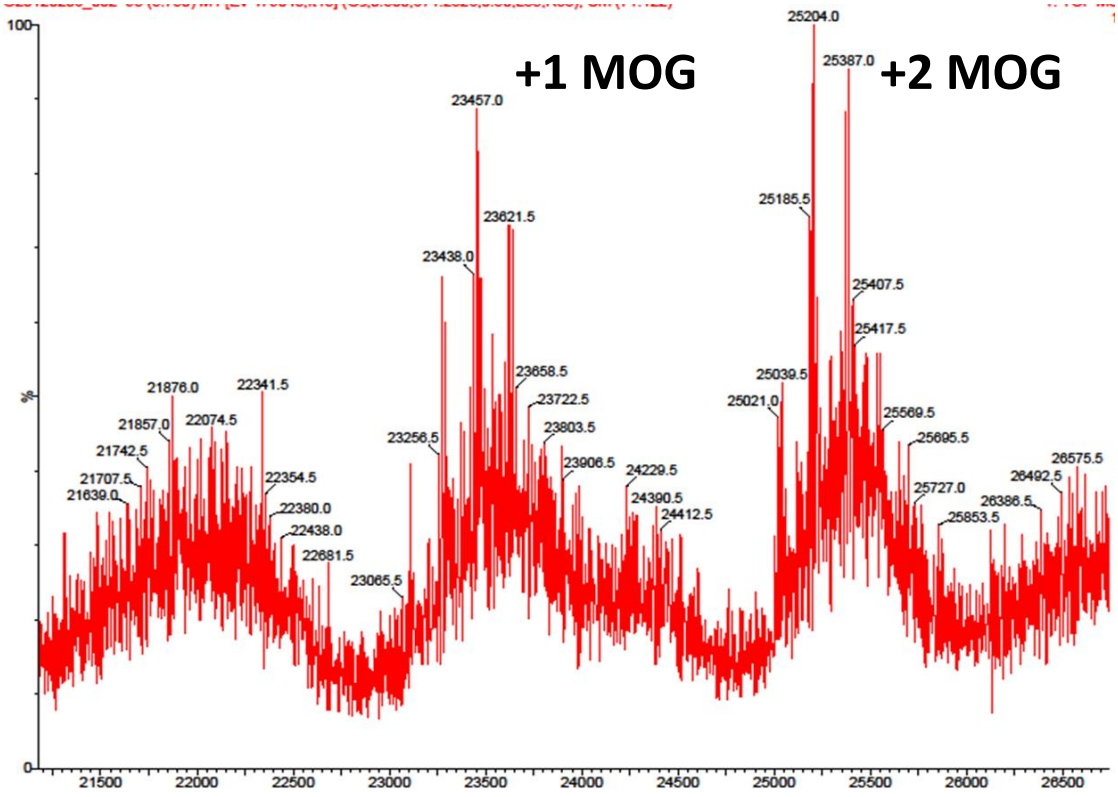

Figure 2.8. Mass spectra of MOG-IDAC. MALDI-TOF mass spectrum of MOG-IDAC conjugates with one or two peptides per molecule I-domain.

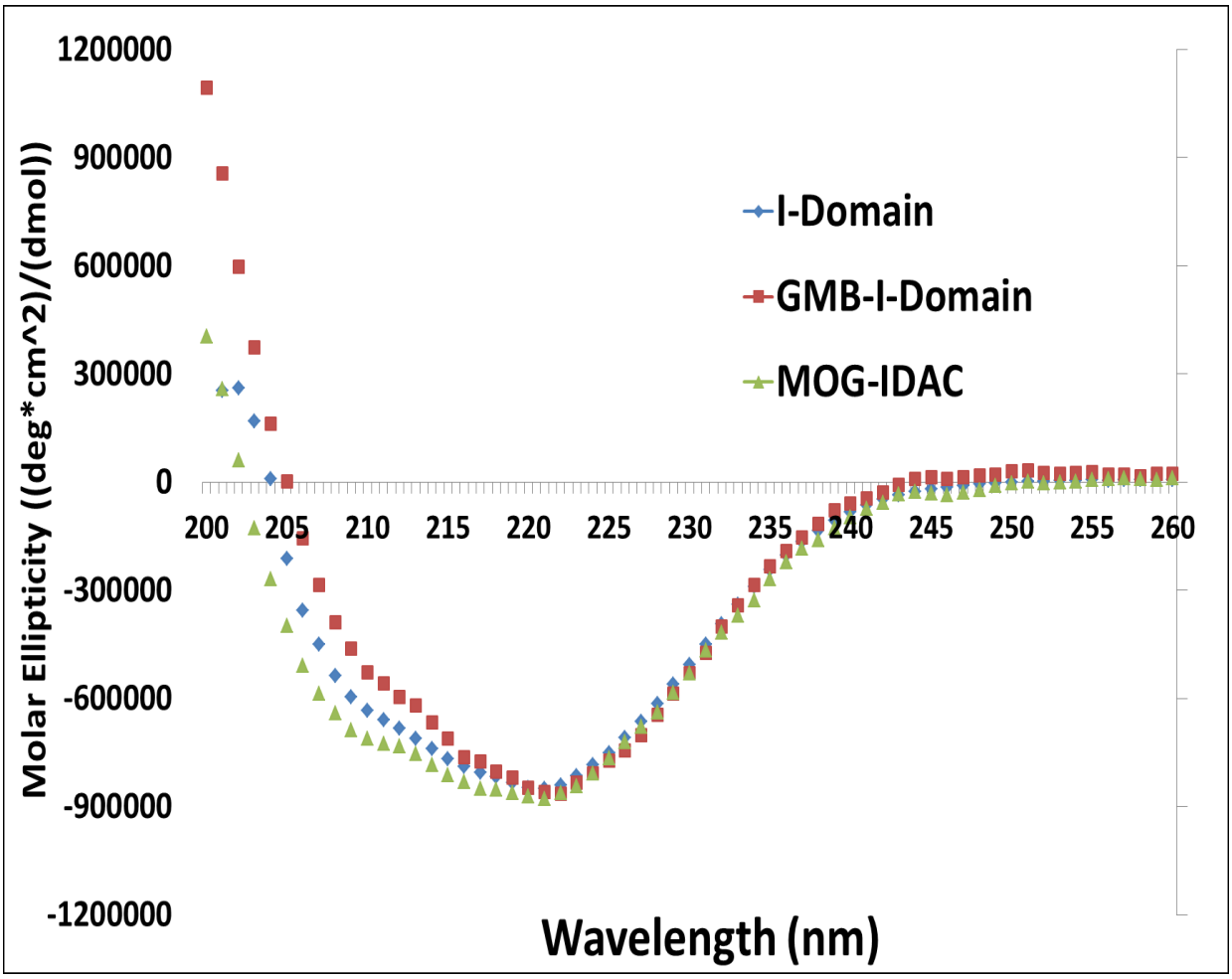

Figure 2.9. CD Spectra of MOG-IDAC. Comparison of CD spectra of parent I-domain (Blue), GMB-I-domain (Red), and MOG-IDAC (Green). The spectrum of MOG-IDAC was not dramatically altered upon peptide conjugation, suggesting that the I-domain in the conjugate maintains its secondary structure.

2.3.3. Synthesis of MOG-PEG-IDAC. The problem in synthesizing MOG-IDAC molecule is that the MOG peptide was insoluble limiting the conjugation efficiency. In an attempt to increase the solubility of the peptide, two poly-ethylene glycol amino acids (i.e., 11-amino-3,6,9-trioxaundecanoic acid) (Figure 2.10) were inserted between the C-terminus of the MOG peptide and the cysteine C-terminal amino acid to give MOG-PEG-Cys peptide. Conjugation of the MOG-PEG-Cys to GMB-I-Domain was completed in the same manner as MOG-IDAC; the reaction yielded the MOG-PEG-IDAC conjugate. The molecule was purified with SEC (Figure 2.11) and SDS-PAGE of the pure product of MOG-PEG-IDAC shows a broad band similar to that of MOG-IDAC (Figure 2.12). The number of conjugated peptide was determined by MALDI-TOF MS (Figure 2.13) and there are 1 to 2 conjugated peptide per one molecule of I-domain. CD spectral analysis was carried out to compare the secondary structure of MOG-PEG-IDAC to MOG-IDAC, GMB-I-domain and I-domain (Figure 2.14). There is a change in the secondary structure of MOG-PEG-IDAC compared to that of MOG-IDAC.

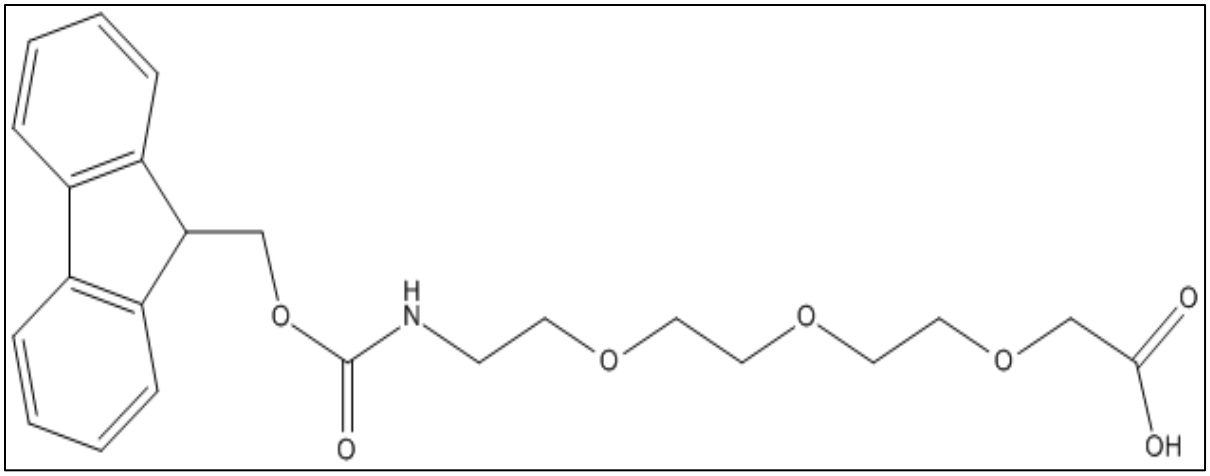

Figure 2.10. Peg linker for MOG-PEG-IDAC. Fmoc-11-amino-3,6,9-trioxaundecanoic acid is the pegylated amino acid used in the synthesis of MOG-PEG-IDAC with a molecular weight of 429.47.

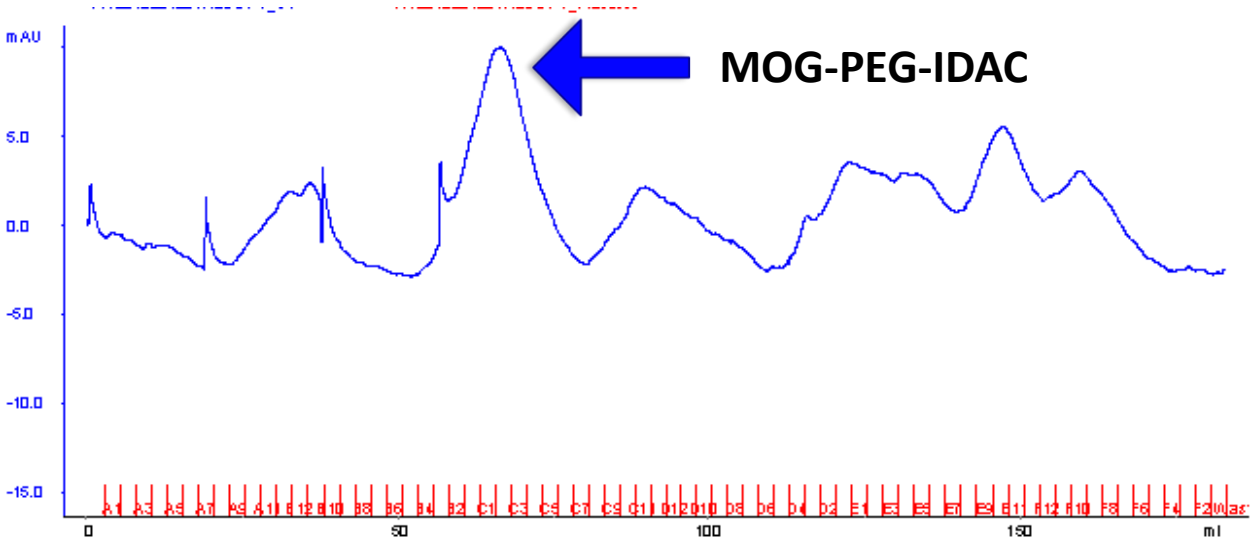

Figure 2.11. SEC Chromatogram of MOG-PEG-IDAC. The SEC chromatogram of MOG-PEG-IDAC appears in a single peak of the conjugate; however, conjugation still yields some protein precipitation. Thus, the amount of protein is solution is low and causes a low absorbance reading of MOG-PEG-IDAC in UV detection during SEC.

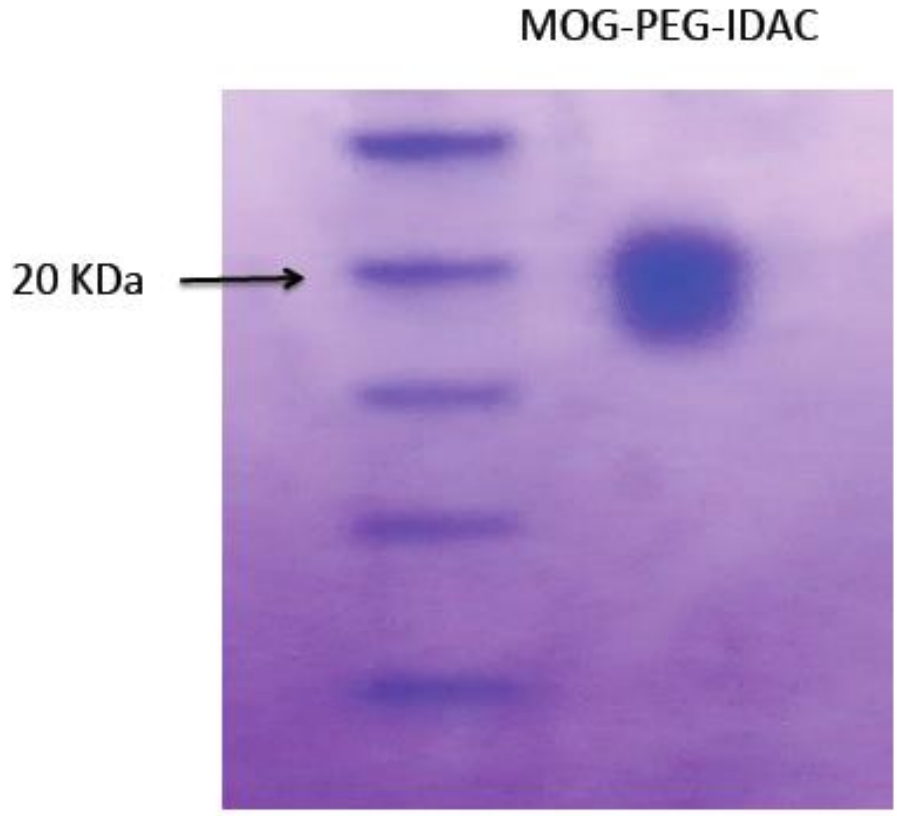

Figure 2.12. SDS PAGE of MOG-PEG-IDAC. Shows a broad band of the desired product without the presence of precursor MOG-PEG-Cys peptide.

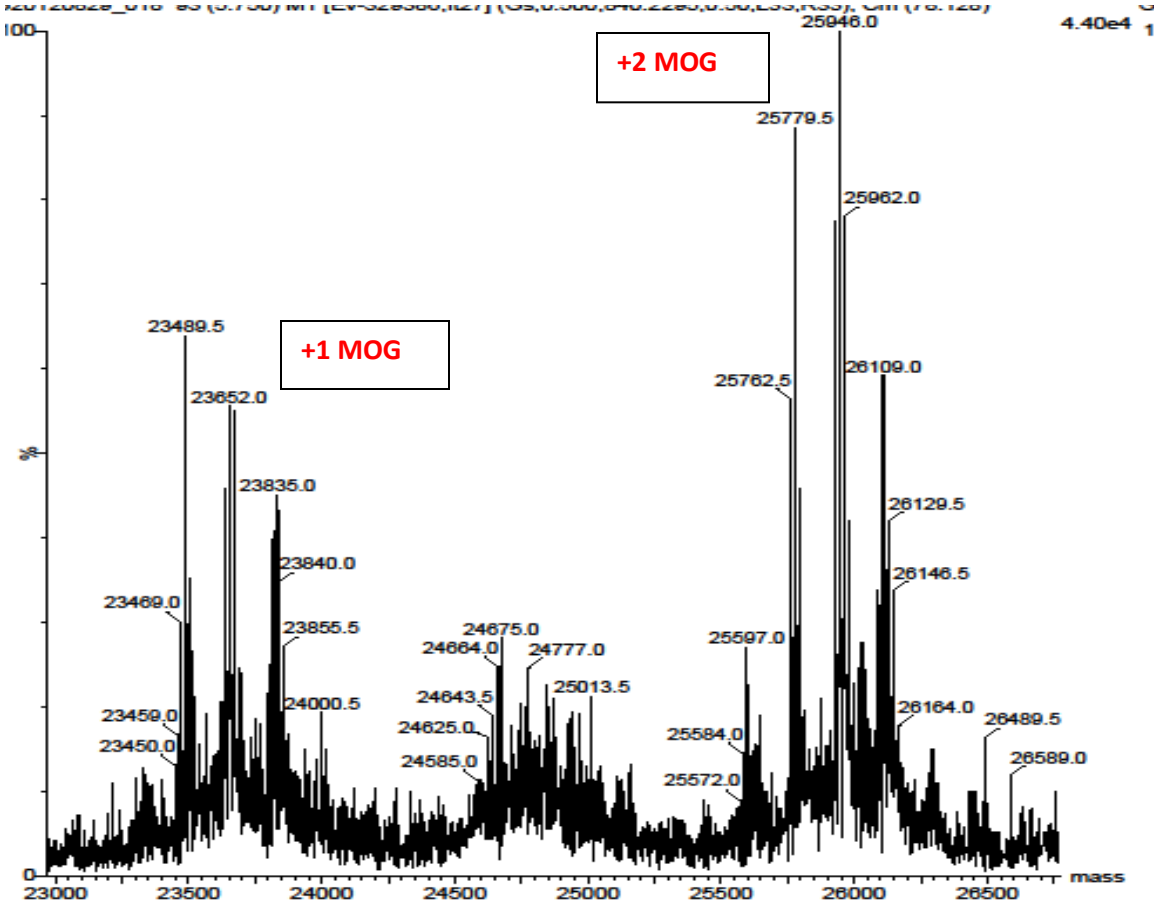

Figure 2.13. Mass Spectrum of MOG-PEG-IDAC. The mass spectrum of MOG-PEG-IDAC to indicate that there are one to two peptides conjugated to the I-domain.

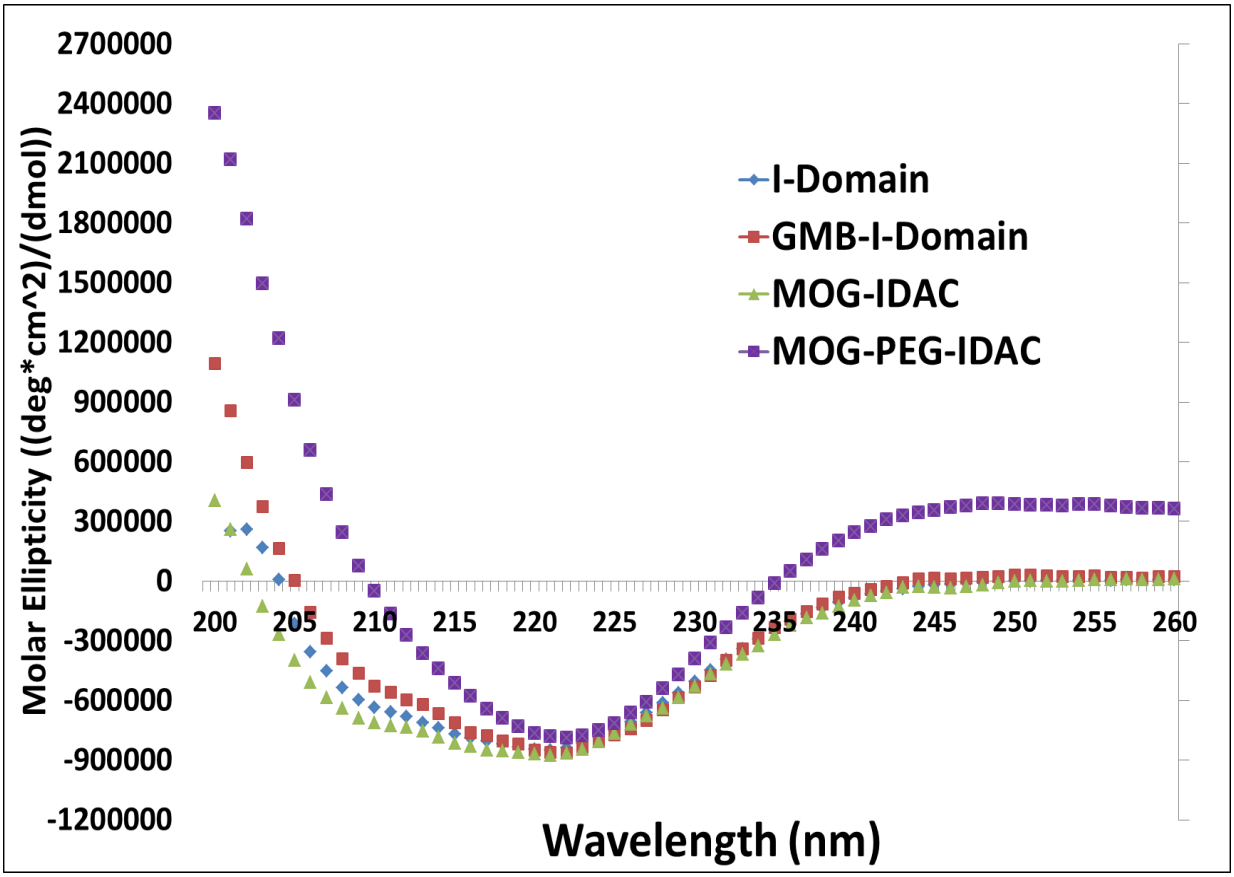

Figure 2.14. CD Spectra of MOG-PEG-IDAC. CD spectra of parent I domain (Blue), GMB-I-Domain (Red), MOG-IDAC (Green), MOG-PEG-IDAC (Purple). The is a significant change in the CD spectrum of MOG-PEG-IDAC, suggesting there is alteration of the secondary structure of the conjugate.

2.4. Discussion

Today, patients with autoimmune diseases such as rheumatoid arthritis, multiple sclerosis, and psoriasis are currently being treated with protein derived drugs such as peptide and monoclonal antibodies to modulate their immune systems. Multiple sclerosis patients are currently being treated with Copaxone® and Tysabri®, along with other anti-inflammatory agents (e.g., mitoxantrone, and Beta-interferon 1a). One common monoclonal antibody treatment is Tysabri, which binds to the α4 subunit of the α4β1 and α4β7 integrins on the surface of leukocytes.

Blocking of the α4 subunit prevents leukocyte adhesion to endothelial cells and subsequent infiltration of T cells and other immune cells into the CNS. Unfortunately, some patients treated with Tysabri have develop progressive multifocal leukoencephalopathy (PML) conditions, a life threatening complication with no available cure [14]. A monoclonal antibody, Raptiva (Efalizumab, CD11a mAB) for cell adhesion molecules has been used to treat psoriasis but due to PML complications, this drug was withdrawn from the U.S. market [28, 29]. In addition to blocking T-cell adhesion to endothelial cells, Tysabri and Raptiva can also block signal-2 recognition between the APC and T-cell. As a result, it may cause a general suppression of T-cell activation and prevents T-cells from responding to pathogens like JC virus which is responsible for the appearance of PML. With this knowledge, there is a need to develop a new therapy that does not suppress the general immune response but is more specific to regulating a certain population of immune cells.

To generate a more antigen-specific immune suppression, our group has developed the BPI molecules such as PLP-BPI, GAD-BPI, and CII-BPI that suppress MS, type 1 diabetes, and

rheumatoid arthritis in animal models [2, 17, 20-22]. In conjunction with the BPI molecules, PLP-IDAC molecules were also developed with several antigenic PLP peptides to a single I-domain [25]. Following induction with one antigen, the disease could exacerbate to include multiple antigens and this phenomenon is termed "antigenic spreading" [30]. The hope is that IDAC can deliver multiple and different antigenic peptides from different myelin sheath proteins (i.e., PLP, MOG, and MBP) for preventing antigenic spreading in autoimmune diseases. Thus, it may provide a unique approach to treating MS. Another advantage is that both BPI and IDAC molecules has been shown to suppress the disease when administered as "vaccine like" treatments; in this case, the molecules are delivered several days before induction of the disease [25]. The proposed mechanism of action of PLP-IDAC molecules is similar to that of BPI molecule in which they inhibit the formation of the immunological synapse by simultaneous binding to ICAM-1 and MHC-II on the surface of APC. This inhibition prevents the activation of T cell and/or alters the differentiation of inflammatory to regulatory T cells.

Although MOG-IDAC was successfully produced, the production yield was very low and was not sufficient quantity for animal studies. However, the amount was sufficient to characterized the molecules by SDS-PAGE, mass spectrometry, and CD spectroscopy [25]. The difficulty of producing MOG-IDAC was due to the insolubility of MOG-Cys peptide to make the reaction with GMB-I-domain inefficient. In this case, MOG-Cys peptide had to be dissolved in DMSO before adding to the reaction mixture for conjugation. This conjugation reaction was less efficient than conjugation between PLP-Cys and GMB-I-domain to make PLP-IDAC. Different reaction conditions were explored including changing the pH and buffers to improve the efficiency of the reaction; unfortunately, none of the change resulted in improved reaction efficiency to make MOG-IDAC. The best reaction condition was by adding the dissolved MOG

peptide in DMSO drop wise to the GMB-I-domain reaction mixture. At pH 7.4, the reaction mixture still produces slight cloudiness in the solution; however, upon filtration, the filtrate showed successful conjugation in SEC. This inefficiency was also reflected by the low number of peptide conjugated to the I-domain in MOG-IDAC compared to PLP-IDAC. It should be noted that the PLP-IDAC has a maximum of five peptides per-molecule of I-domain. It is interesting to find that adding MOG peptides did not dramatically alter the CD spectra MOG-IDAC compared to the I-domain, suggesting that the MOG peptide has low contribution to the secondary structure of the conjugates. Due to the difficulty of producing sufficient quantity, the animal studies were not carried out with MOG-IDAC.

To improve the synthesis of the conjugate, solubility of the peptide was improved by adding PEG groups between MOG peptide and the cysteine residue to make MOG-PEG-Cys. It has been shown that PEGylation of proteins and peptides improves the biopharmaceutical properties, through increase in solubility, increase in half-life, and decrease in immunogenicity [31, 32]. PEGylation has been shown to be safe and non-toxic. For example, certolizumab pegol is a TNFα antibody; this molecule is a humanized Fab' antibody fragment conjugated to PEG to increase the half-life and decrease immunogenicity [33]. This drug has been used in the clinic for the treatment of RA. Our group had also utilized PEG group as a linker to make PLP-PEG-BPI and the use of PEG in PLP-PEG-BPI lowered the anaphylaxis incidence compared to PLP-BPI molecules in the EAE mouse model [21]. Besides increasing solubility, the hope is that adding PEG groups as a linker could also lower the toxicity profile (i.e., anaphylaxis reaction) of MOG-PEG-IDAC [25]. Unfortunately, the solubility of MOG-PEG-IDAC was still not improved tremendously compared to MOG-IDAC because precipitation was still observed during conjugation reaction at neutral pH. The secondary structure of MOG-PEG-IDAC was also

altered to increase the beta-sheet structure compared to the MOG-IDAC and the I-domain as shown in the CD spectra (Figure 2.13). The beta-sheet structure in the MOG-PEG-IDAC may lead to aggregation of the conjugate, contributing to the insolubility of the MOG-PEG-IDAC. It is not clear whether the increase in beta sheet structure is due to the contribution of the MOG peptide to the secondary structure of the conjugate or it is due to the change of random coil or alpha helix structure to beta sheet within the I-domain protein of the conjugate. In the future, further studies will be carried out to evaluate the effect of MOG peptide on the secondary structure of the IDAC.

In conclusion, we have developed a new IDAC molecule (MOG-IDAC and MOG-PEG-IDAC) and successfully managed to purify and characterize it using SEC, SDS-PAGE, Mass Spectrometry, and CD. In the future, there will be a need to improve the efficiency of the conjugation reaction in order to progress to proof-of-concept of the MOG-PEG-IDAC in EAE animal models for suppression of disease. The efficacy of MOG-PEG-IDAC in suppressing EAE is currently being studies in the MOG-stimulated EAE in C57BL/6 mice. The effect of the conjugate in altering the cytokine production will also be determined. Furthermore, the physical, chemical, and plasma stability of the conjugates will be investigated in the future.

2.5. References

1. Fletcher JM, Lalor SJ, Sweeney CM, Tubridy N, Mills KH. T cells in multiple sclerosis and experimental autoimmune encephalomyelitis. Clin Exp Immunol. 2010; 162: 1–11.

2. Kobayashi N, Kobayashi H, Gu L, Malefyt T, Siahaan TJ. Antigen-specific suppression of experimental autoimmune encephalomyelitis by a novel bifunctional peptide inhibitor. J Pharmacol Exp Ther. 2007; 322: 879–886.

3. Serafini B, Severa M, Columba-Cabezas S, Rosicarelli B, Veroni C, Chiappetta G, Magliozzi R, Reynolds R, Coccia EM, Aloisi F. Epstein-Barr virus latent infection and BAFF expression in B cells in the multiple sclerosis brain: implications for viral persistence and intrathecal B-cell activation. J Neuropathol Exp Neurol. 2010; 69: 677–693.

4. Ebers GC. Environmental factors and multiple sclerosis. Lancet Neurology. 2008; 7: 268–277.

5. Haines JL, Ter-Minassian M, Bazyk A, Gusella JF, Kim DJ, Terwedow H, Pericak-Vance MA, Rimmler JB, Haynes CS, Roses AD, Lee A, Shaner B, Menold M, Seboun E, Fitoussi RP, Gartioux C, Reyes C, Ribierre F, Gyapay G, Weissenbach J, Hauser SL, Goodkin DE, Lincoln R, Usuku K, Oksenberg JR, et al. A complete genomic screen for multiple sclerosis underscores a role for the major histocompatability complex. The Multiple Sclerosis Genetics Group. Nat Genet. 1996; 13: 469–471.

6. Mohr DC, Hart SL, Julian L, Cox D, Pelletier D. Association between stressful life events and exacerbation in multiple sclerosis: a meta analysis. British Medical Journal. 2004; 328: 731–736.

7. Whitacre CC. Sex differences in autoimmune disease. Nat Immunol. 2001; 2: 777–780.

8. Manikwar P, Kiptoo P, Badawi AH, Buyuktimkin B, Siahaan TJ. Antigen-specific blocking of CD4-specific immunological synapse formation using BPI and current therapies for autoimmune diseases. Med Res Rev. 2012; 32: 727–764.

9. Matsushita T, Yanaba K, Bouaziz JD, Fujimoto M, Tedder TF. Regulatory B cells inhibit EAE initiation in mice while other B cells promote disease progression. J Clin Invest. 2008; 118: 3420–3430.

10. Kappos L, Antel J, Comi G, Montalban X, O'Connor P, Polman CH, Haas T, Korn AA, Karlsson G, Radue EW. Oral fingolimod (FTY720) for relapsing multiple sclerosis. New Engl J Med. 2006; 355: 1124–1140.

11. Arnon R. The development of Cop 1 (Copaxone®), and innovative drug for the treatment of multiple sclerosis personal reflections. Immunol Lett. 1996; 50: 1–15.

12. Marriott JJ, Miyasaki JM, Gronseth G, O'Connor PW. Evidence Report: The efficacy and safety of mitoxantrone (Novantrone) in the treatment of multiple sclerosis. Report of the Therapeutics and Technology Assessment Subcommittee of the American Academy of Neurology. Neurology. 2010; 74: 1463–1470.

13. Cadavid D, Wolansky LJ, Skurnick J, Lincoln J, Cheriyan J, Szczepanowski K, Kamin SS, Pachner AR, Halper J, Cook SD. Efficacy of treatment of MS with IFN beta-1b or

glatiramer acetate by monthly brain MRI in the BECOME study. Neurology. 2009; 72: 1976–1983.

14. Goodin DS, Cohen BA, O'Connor P, Kappos L, Stevens JC. Assessment: The use of natalizumab (Tysabri) for the treatment of multiple sclerosis (an evidence-based review) - Report of the therapeutics and technology assessment subcommittee of the American Academy of Neurology. Neurology. 2008; 71: 766–773.

15. Kress-Bennett JM, Ehrlich GD, Bruno A, Post JC, Hu FZ, Scott TF. Preliminary study: treatment with intramuscular interferon beta-1a results in increased levels of IL-12Rbeta2+ and decreased levels of IL23R+ CD4+ T - Lymphocytes in multiple sclerosis. BMC Neurol. 2011; 11: 155.

16. Badawi AH, Kiptoo P, Wang WT, Choi IY, Lee P, Vines CM, Siahaan TJ. Suppression of EAE and prevention of blood-brain barrier breakdown after vaccination with novel bifunctional peptide inhibitor. Neuropharmacology. 2012; 62: 1874–1881.

17. Murray JS, Oney S, Page JE, Kratochvil-Stava A, Hu Y, Makagiansar IT, Brown JC, Kobayashi N, Siahaan TJ. Suppression of type 1 diabetes in NOD mice by bifunctional peptide inhibitor: modulation of the immunological synapse formation. Chem Biol Drug Des. 2007; 70: 227–236.

18. Badawi AH, Siahaan TJ. Immune modulating peptides for the treatment and suppression of multiple sclerosis. Clin Immunol. 2012; 144: 127–138.

19. Buyuktimkin B, Wang Q, Kiptoo P, Stewart JM, Berkland C, Siahaan TJ. Vaccine-like controlled-release delivery of an immunomodulating peptide to treat experimental autoimmune encephalomyelitis. Mol Pharm. 2012; 9: 979–985.

20. Kobayashi N, Kiptoo P, Kobayashi H, Ridwan R, Brocke S, Siahaan TJ. Prophylactic and therapeutic suppression of experimental autoimmune encephalomyelitis by a novel bifunctional peptide inhibitor. Clin Immunol. 2008; 129: 69–79.

21. Ridwan R, Kiptoo P, Kobayashi N, Weir S, Hughes M, Williams T, Soegianto R, Siahaan TJ. Antigen-specific suppression of experimental autoimmune encephalomyelitis by a novel bifunctional peptide inhibitor: structure optimization and pharmacokinetics. J Pharmacol Exp Ther. 2010; 332: 1136–1145.

22. Zhao H, Kiptoo P, Williams TD, Siahaan TJ, Topp EM. Immune response to controlled release of immunomodulating peptides in a murine experimental autoimmune encephalomyelitis (EAE) model. J Control Release. 2010; 141: 145–152.

23. Schmidt S. Candidate autoantigens in multiple sclerosis. Multiple sclerosis. 1999; 5: 147–160.

24. Higgins PJ, Weiner HL. Suppression of experimental autoimmune encephalomyelitis by oral administration of myelin basic protein and its fragments. J Immunol. 1988; 140: 440–445.

25. Manikwar P, Buyuktimkin B, Kiptoo P, Badawi AH, Galeva NA, Williams TD, Siahaan TJ. I-domain-antigen conjugate (IDAC) for delivering antigenic peptides to APC:

synthesis, characterization, and in vivo EAE suppression. Bioconjug Chem. 2012; 23: 509–517.

26. Büyüktimkin B, Manikwar P, Kiptoo PK, Badawi AH, Jr. JMS, Siahaan TJ. Vaccine-like and Prophylactic Treatments of EAE with Novel I-Domain Antigen Conjugates (IDAC): Targeting Multiple Antigenic Peptides to APC. Mol Pharm. 2012; November.

27. Zimmerman T, Oyarzabal J, Sebastian ES, Majumdar S, Tejo BA, Siahaan TJ, Blanco FJ. ICAM-1 peptide inhibitors of T-cell adhesion bind to the allosteric site of LFA-1. An NMR characterization. Chem Biol Drug Des. 2007; 70: 347–353.

28. Carson KR, Focosi D, Major EO, Petrini M, Richey EA, West DP, Bennett CL. Monoclonal antibody-associated progressive multifocal leucoencephalopathy in patients treated with rituximab, natalizumab, and efalizumab: a Review from the Research on Adverse Drug Events and Reports (RADAR) Project. Lancet Oncol. 2009; 10: 816–824.

29. Pugashetti R, Koo J. Efalizumab discontinuation: a practical strategy. J Dermatolog Treat. 2009; 20: 132–136.

30. McRae BL, Vanderlugt CL, Dal Canto MC, Miller SD. Functional evidence for epitope spreading in the relapsing pathology of experimental autoimmune encephalomyelitis. J Exp Med. 1995; 182: 75–85.

31. Mehvar R. Modulation of the pharmacokinetics and pharmacodynamics of proteins by polyethylene glycol conjugation. J Pharm Pharm Sci. 2000; 3: 125–136.

32. Caliceti P, Veronese FM. Pharmacokinetic and biodistribution properties of poly(ethylene glycol)-protein conjugates. Adv Drug Deliv Rev. 2003; 55: 1261–1277.

33. Barnes T, Moots R. Targeting nanomedicines in the treatment of rheumatoid arthritis: focus on certolizumab pegol. Int J Nanomedicine. 2007; 2: 3–7.

Chapter 3

Suppression of EAE using vaccine-like treatment with PLP-PEG-B7AP

3.1. Introduction

Multiple sclerosis (MS), an autoimmune neurological disease, is difficult to treat because it involves the destruction of the myelin sheath of the axon connecting the nerve cells in the central nervous system (CNS) [1, 2]. In the disease pathogenesis, the immune cells recognize the major self-proteins on the myelin sheath, including proteolipid protein (PLP), myelin oligodendrocyte glycoprotein (MOG), and myelin basic protein (MBP) [3]. For T-cell activation and modulation, TCR/MHC-II-Ag complex (Signal-1) and costimulatory signal (Signal-2) are generally required during the interaction between T cells and antigen-presenting cells (APC) [4]. The positive costimulatory signals can be delivered by CD28/B7 interactions (B7 on APC and CD28 on T cells) [5, 6]. In contrast, the negative costimulatory signal can be delivered by B7/CTLA-4 [7].

The CD28 protein on CD4+ T cells binds to the B7.1 and B7.2 receptors on APC via a conserved region with MYPPPY sequence [8, 9]. B7AP peptide containing the conserved MYPPPY sequence can bind to B7 receptors and block CD28/B7 interactions without affecting the B7/CTLA-4 interactions [10]. Blocking C28/B7 interactions with B7AP peptide has been shown to prevent rejection of organ transplants in an animal model [10]. Another peptide called EL-CD28 that has the MYPPPY sequence was also shown to suppress experimental autoimmune encephalomyelitis (EAE) in an animal model [6]. It has been proposed that blocking the specific binding of the MYPPPY region of CD28 to both B7.1 and B7.2 receptors can induce T-cell anergy for suppression of the immune response [11-14]. In the animal studies, administration of anti-B7.1 antibody that recognizes the binding site of MYPPPY sequence of CD 28 can induce exacerbation of diabetes in non-obese diabetic mice, suggesting that CD28/B7 costimulatory interaction is important for inducing T-cell activation. [11].

Interactions between cell adhesion molecules such as intercellular adhesion molecule-1 (ICAM-1) and leukocyte function-associated antigen-1 (LFA-1) play an important role in the formation of the immunological synapse for T-cell activation [15, 16]. Our previous findings show that novel bifunctional peptide inhibitor (BPI) molecules that are a conjugate between antigenic peptide(s) and cell adhesion peptide(s) from the ICAM-1 or LFA-1 sequence can effectively suppress EAE in the mouse model [2, 17, 18]. The proposed mechanism of BPI molecules is that they block immunological synapse formation and stop the activation of a specific population of immune cells; therefore, they avoid the general suppression of immune cells [2, 18]. It is believed that this type of treatment has an advantage over treatments with drugs that suppress the general immune response. Recently, another type of BPI molecule called PLP-B7AP was developed with B7AP peptide from the sequence of costimulatory signal CD28. In this case, PLP-B7AP is hypothesized to block signal-1 (MHC-II/TCR) and signal-2 (CD28/B7) and prevent PLP-specific T-cell activation. A very effective suppression of EAE was achieved using PLP-B7AP in treatment on days 4, 7, and 10 following induction of disease at day 0.

The EAE animal model has been used to better understand the pathogenesis of MS and to develop new strategies for the treatment of MS. The pathogenesis EAE model is similar to MS in that it is characterized by inflammation of the CNS, breakdown of the blood-brain barrier (BBB), and differentiation and proliferation of the T_H17 and T_H1 cells [15]. To prevent the disease, the pro-inflammatory and inflammatory T cells must be suppressed and/or regulated by increasing the differentiation and proliferation of regulatory cells (T_{reg}) [19] and suppressor type-2 helper T cells (T_H2) [20]. Leakiness of the BBB increases in EAE as well as in MS, allowing trafficking of leukocytes into the CNS and the subsequent destruction of myelin sheaths [21-23]. Our previous studies have demonstrated that the BPI molecule administered in a "vaccine-like"

manner can suppress EAE in mice and prevent BBB breakdown as analyzed by magnetic resonance imaging (MRI) [24].

In this study, a derivative of the PLP-B7AP molecule called PLP-PEG-B7AP was synthesized by conjugating $PLP_{139-151}$ peptide to the B7AP peptide from CD28 via a pegylated amino acid linker. PLP-PEG-B7AP is hypothesized to block the interactions of the primary MHC-II/TCR signal and secondary CD28/B7) signal to prevent activation of T cells followed by suppression of EAE progression in the animal model. This also demonstrates the importance of the CD28/B7 costimulatory signal in the activation of T-cells during autoimmunity. PLP-PEG-B7AP was injected subcutaneously (s.c.) in a vaccine-like manner, and disease scores, changes in body weight, and incidence of disease were monitored. Cytokine levels produced by splenocytes on days 15 and 30 were monitored and analyzed to determine the populations of T cells that are proliferating during progression of the disease. Brain samples of mice from days 15 and 30 were analyzed for leukocyte infiltrations (i.e., CD3+ T cells) and amount of demyelination of the CNS.

3.2. Experimental Procedures

3.2.1. Mice. The University of Kansas Institutional Animal Care and Use Committee (IACUC) approved all protocols for animal experiments using SJL/J($H\text{-}2^s$) mice (Charles River, Wilmington, MA). The Animal Care Unit facility at The University of Kansas housed the mice under the supervision of veterinarians; the facility is approved by the Association for Assessment and Accreditation of Laboratory Animal Care.

3.2.2. Peptide synthesis. The crude peptides such as $PLP_{139-151}$ (Ac-HSLGKWLGHPDKF-NH_2), PLP-BPI (Ac-HSLGKWLGHPDKF-$(Acp\text{-}G\text{-}Acp\text{-}G\text{-}Acp)_2$-ITDEATDSG-$NH_2$), and PLP-PEG-B7AP (Ac-HSLGKWLGHPDKF-$(PEG)_3$-G-$(PEG)_3$-EFMYPPPYD-NH_2) were synthesized by Shanghai Mocell Biotech Co., Shanghai, China. A list of peptides can be found in table 3.1. The crude peptides were purified by reversed-phase high performance liquid chromatography (RP-HPLC) on a semi-preparative C18 column with a gradient of solvent A (94.5% H_2O, 5% acetonitrile, 0.1% TFA) and solvent B (100% acetonitrile). The purity of each fraction from semi-preparative HPLC was evaluated using analytical RP-HPLC (C18 column) and all pure fractions were pooled and subjected to lyophilization. The identity of each purified peptide was confirmed by electrospray ionization mass spectrometry.

Peptide	**Sequence**	**Molecular Weight**
PLP	Ac-HSLGKWLGHPDKF-NH2	1665.965
PLP-BPI	Ac-HSLGKWLGHPDKF-Acp-G-Acp-G-Acp-Acp-G-Acp-G-Acp-ITDGEATDSG-NH2	3416.91
PLP-PEG-B7AP	Ac-HSLGKWLGHPDKF-PEG3-G-PEG3-EFMYPPPYD-NH2	4008.33

Table 3.1 Peptides used. Listed table of peptides and their sequences used in current study.

3.2.3. Vaccine-like treatment of EAE with peptides. Prior to disease induction, four groups of SJL/J female mice (5–7 weeks) received three s.c. injections of either 100 µl of PBS or 100 µl (100 nmol/injection/day) of PLP-PEG-B7AP, PLP-BPI, and PLP peptides at 11, 8, and 5 days

prior to induction of disease on day 0. On day 0, the mice then were immunized s.c. with 200 µg of PLP in a 0.2 ml emulsion that contained equal volumes of PBS and complete Freund's adjuvant (CFA) containing killed mycobacterium tuberculosis strain H37RA at a final concentration of 8 mg/ml (Difco, Detroit, MI). 50 µl of PLP/CFA emulsion was administered to regions above the shoulder and the flanks (total of 4 sites). In addition, 200 ng of pertussis toxin (List Biological Laboratories, Campbell, CA) was delivered intraperitoneally (i.p.) on days 0 and 2. The disease progression was measured by clinical scores using the following scoring system: 0 = no clinical symptoms, 1 = limp tail or waddling gait with tail tonicity; 2 = waddling gait with limp tail (ataxia); 3 = full paralysis of one limb; 4 = full paralysis of two limbs; 5 = moribund or dead. The body weight of each animal was determined daily.

3.2.4. Cytokine production assay. In vitro cytokine assays were performed following a protocol that was described previously [24]. Briefly, spleens were isolated from 3 animals treated with PLP-PEG-B7AP and PBS on days 15 (at the highest disease score) and 30 (at remission). Splenocytes were harvested by mashing the spleen and running the cells through a cell strainer in serum-free RPMI-1640 medium. ACK lysis buffer (Invitrogen, Carlsbad, CA) was use to remove the red blood cells. Serum-free RPMI-160 medium (Cellgro, Manassas, VA) was used to wash the remaining splenocytes. The cells were placed in each well of a 24-well plate with a density of 5×10^6 cells/well and primed with PLP (20 µM). After 72 h, the supernatants from each well were collected and stored in a –80°C freezer for up to 78 hours until cytokine analysis to measure IL-2, IL-4, IL-5, IL-6, IL-10, IL-17, and IFN-γ using a quantitative ELISA-based Q-Plex assay (Quansys Biosciences, Logan, UT).

3.2.5. Brain tissue staining and analysis. Brain tissue was isolated at the same time as the isolation of spleens. After isolation, the brain tissue was placed in a cold solution of 4% paraformaldehyde for 48 hours at 4°C. The brain tissue was then rinsed 3 times with PBS and then stored in 70% ethanol until it was processed into paraffin blocks. Processing of brain tissue was completed at the University of Kansas Medical Center by immersing the brain tissue in a gradient of ethanol (70–100%), xylene, and then Paraplast X-tra®. The brain tissue was then placed in cooled paraffin blocks followed by sectioning. Samples were stained for extent of leukocyte infiltration (H&E staining), demyelination (Luk Sol Fast staining), and T-cell infiltration (CD3+ antibody staining). Staining and analysis were done by IHC World, LLC (Woodstock, MD).

3.2.6. Statistical analysis. Statistical analysis was done using one-way analysis of variance followed by Fisher's least significance difference to compare the different parameters, including EAE clinical scores, changes in body weight, and in vitro cytokine production. All statistical analyses were performed using SigmaPlot software (Systat Software Inc, San Jose, CA).

3.3 Results

It has been previously shown that PLP-B7AP (unpublished) and PLP-BPI molecules have better efficacy in suppressing EAE than does PLP peptide when injected subcutaneously s.c. on days 4, 7, and 10 after disease stimulation using a PLP/CFA emulsion on day 0 [25]. In this

study, the efficacy of PLP-PEG-B7AP as a vaccine was evaluated for suppressing EAE in the mouse model. The PLP-PEG-B7AP peptide was administered via s.c. injections on days –11, –8, and –5 prior to stimulation of disease on day 0 with PLP/CFA emulsion.

3.3.1. Suppression of EAE with PLP-PEG-B7AP. Disease progression and severity were measured using a standard disease scoring protocol (Figure3.1), in which scores can range from 0 to 5. The first evidence of disease was found in PBS- and PLP-treated mice on days 10 and 11. The disease became severe between days 13 and 16 with a maximum average disease score on day 15 of 2.50 ± 0.274 for PBS-treated and 2.00 ± 0.315 for PLP-treated mice (n = 6 for each group). After the disease peaked, all the mice slowly underwent remission. Half of the PLP-BPI-treated mice showed signs of disease, which resulted in a maximum average disease score of 1.08 ± 0.153 observed on days 12–14 and 16 (n = 6 for each group). Less than half of the PLP-PEG-B7AP-treated mice showed signs of disease during the study, which resulted in a maximum average disease score of 0.777 ± 0.078 observed on day 13. The results suggest that PLP-PEG-B7AP was able to significantly suppress EAE compared to PBS ($p< 0.0001$), PLP ($p< 0.0001$) and PLP-BPI ($p< 0.0001$).

The efficacy of PLP-PEG-B7AP was also evaluated using percent change in body weight of the mice during progression of disease. Overall, the change in body weight correlates with progression of the disease. PBS-treated mice showed a significant loss in body weight (approximately 17%) ($p< 0.001$) on day 13 when compared to PLP- (~15%) ($p< 0.001$), PLP-BPI- (~10%) ($p< 0.001$), and PLP-PEG-B7AP-treated mice (~5%) ($p< 0.001$) (Figure 3.2) After day 13, it was difficult to compare the body weights because two mice from the PBS-treated

group and one mouse from the PLP-treated group had to be euthanized due to very high disease scores. A summary of the incidence of disease is shown in Figure 3.3.

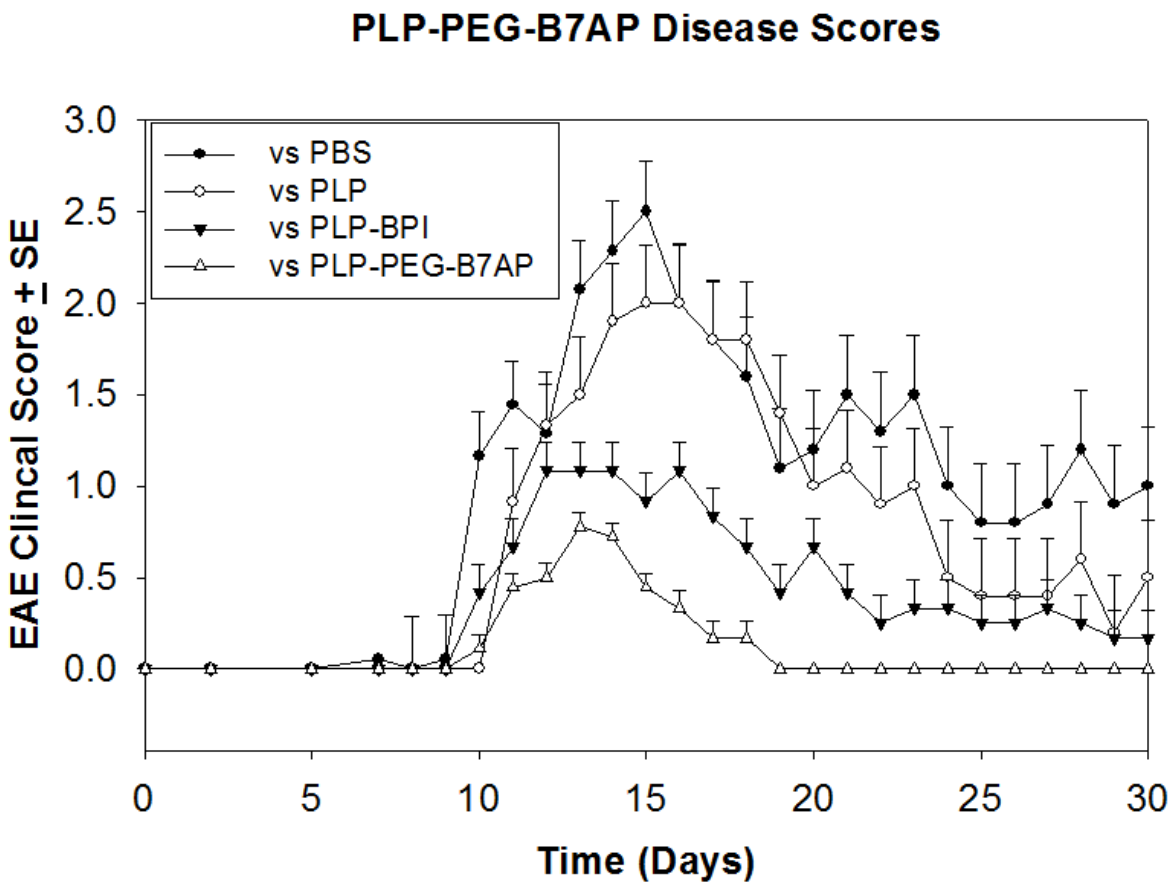

Figure 3.1. Disease Scores of PLP-PEG-B7AP treated mice. In vivo efficacies of PLP-PEG-B7AP, PLP-BPI, PLP, and PBS in suppressing EAE upon vaccination with these compounds on days –11, –8, and –5 followed by immunization with PLP/CFA on day 0. PLP-PEG-B7AP, PLP-BPI, and PLP peptides were administered at a dose of 100 nmol/100 µl/injection. EAE disease scores were significantly lower for PLP-PEG-B7AP (p<0.0001) treated mice than those of PLP-BPI (p<0.0001), PLP (p<0.0001), and PBS(p<0.0001) treated mice.

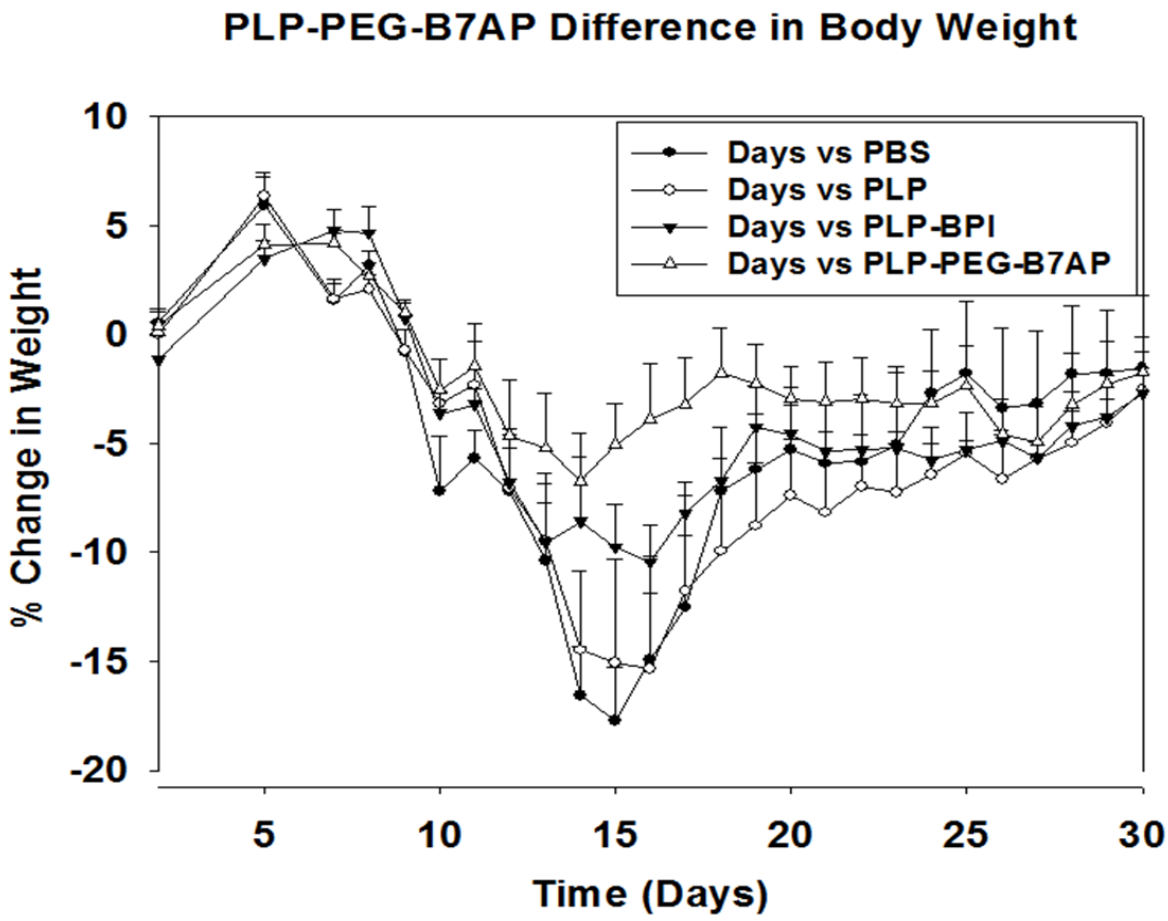

Figure 3.2. Changes in weight of PLP-PEG-B7AP treated Mice. In vivo efficacies of PLP-PEG-B7AP, PLP-BPI, PLP, and PBS were investigated by monitoring the changes in body weight of the animals. Until day 11, PBS (p<0.001)-treated mice demonstrated a significant loss in body weight when compared to PLP (p<0.001), PLP-BPI (p<0.001), and PLP-PEG-B7AP-treated mice (p<0.001). Differences between groups are not so apparent on days 12 and 13, due to the euthanasia of one PLP-treated and two PBS-treated mice. However, the differences in change in body weight become apparent again on days 14 and 15, showing significant loss in body weight in PBS-treated mice compared to PLP-, PLP-BPI-, and PLP-PEG-B7AP-treated mice (p<0.0001).

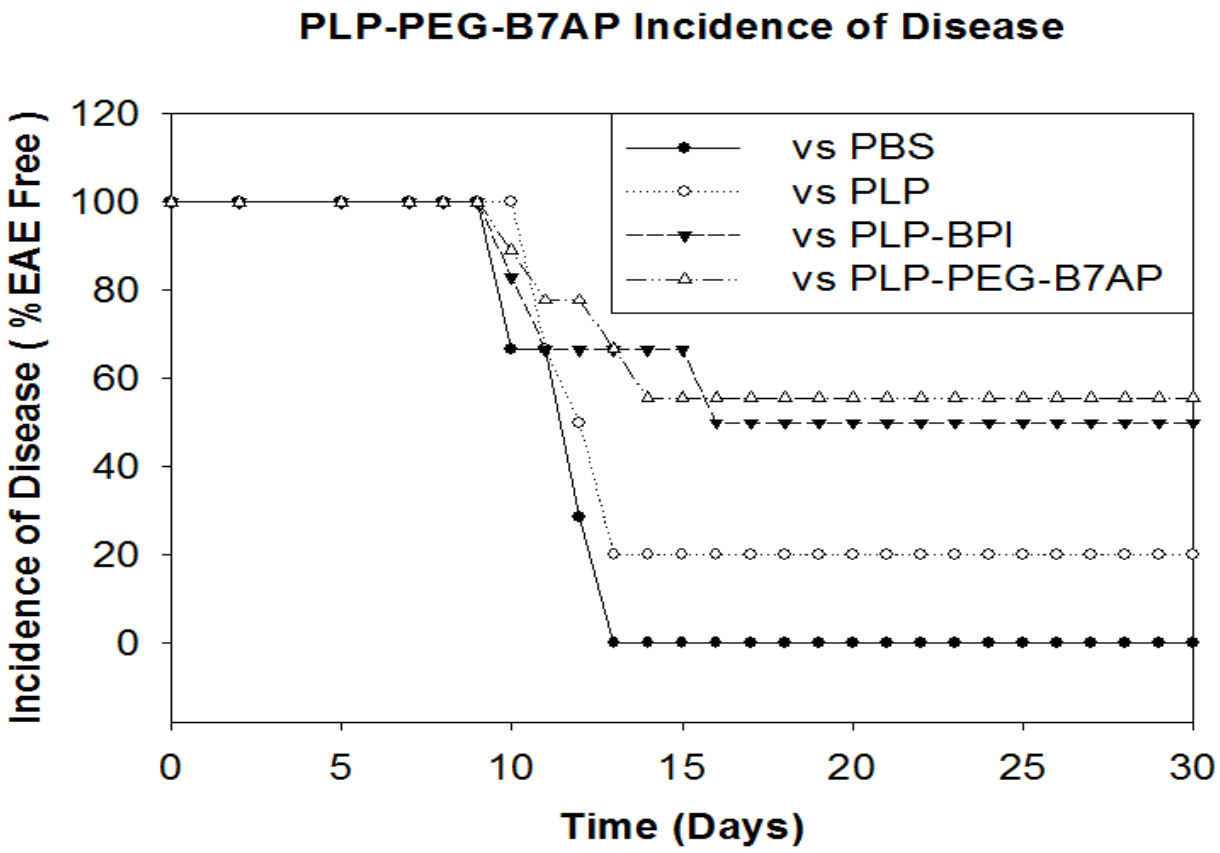

Figure 3.3. Incidence of Disease of PLP-PEG-B7AP treated mice. Disease incidence in EAE mice during in vivo efficacy studies of PLP-PEG-B7AP, PLP-BPI, PLP, and PBS. To be considered to have an incidence of disease, the mouse must have a disease score of one or higher. All of the PBS-treated mice had disease incidence with disease scores of higher than one, and 80% of the PLP-treated mice had the disease. The lowest disease incidences were recorded for the PLP-BPI-treated (66% with scores >1) and PLP-PEG-B7AP-treated (50% with scores > 1) mice.

3.3.2. Splenocyte cytokine production. To better understand the balance between inflammatory and regulatory cells in animals treated with PLP-PEG-B7AP, splenocytes were isolated from both PLP-PEG-B7AP- and PBS-treated mice on days 15 and 30. The types and levels of cytokines secreted by splenocytes provide evidence for the presence of certain types of immune cells upon treatment with the peptide. Although this method will not indicate the concentration of cytokines in systemic circulation, it will provide an idea of relative levels of proliferation of inflammatory and regulatory cells. With an inflammatory response, we expect a greater production of pro-inflammatory cytokines (IL-6, IL-17 and IFN-γ). If there were an activation of regulatory and suppressor immune response, there would be a greater concentration of regulatory cytokines (IL-2, IL-10) and suppressor cytokines (IL-5 and IL-4) than in the normal condition.

The progression of EAE is thought to be due primarily to activation and proliferation of T_H17 and T_H1 cells. The BPI molecule is hypothesized to induce T-cell anergy and shift the immune system from inflammatory to regulatory/suppressor responses. At day 15 there was no statistical difference in production of inflammatory cytokine IL-6, and only a slight difference in production of inflammatory cytokine IL-17 between PBS and PLP-PEG-B7AP treated groups $P<0.001$(n=3) (Figure 3.4). Interestingly only suppression of inflammatory cytokine IFN-γ is observed in the PLP-PEG-B7AP group in comparison to PBS $P<0.001$ (n=3). Regulatory cytokine IL-2 was produce at similar levels in both PLP-PEG-B7AP and PBS treated groups $P<0.001$ (n=3) (Figure3.5). However suppressor cytokine IL-5 was produced at higher levels in PLP-B7AP treated groups then PBS. While decreased production of regulatory cytokine IL-10 and suppressor cytokine IL-4 were observed in PLP-PEG-B7AP treated groups compared to PBS $P<0.001$ (n=3) (Figure 3.5).

At day 30, it is clear that PLP-PEG-B7AP suppresses the production of inflammatory cytokines IFN-γ, IL-17, and IL-6 $P<0.001$ ($n=3$) (Figure 3.6). In contrast, the regulatory cytokines (IL-2, IL-10) and suppressor cytokine (IL-4) were lower in PLP-PEG-B7AP-treated mice than in PBS-treated mice while there was no difference in IL-5 production between the PLP-PEG-B7AP- and PBS-treated mice $P<0.001$ ($n=3$) (Figure 3.7).

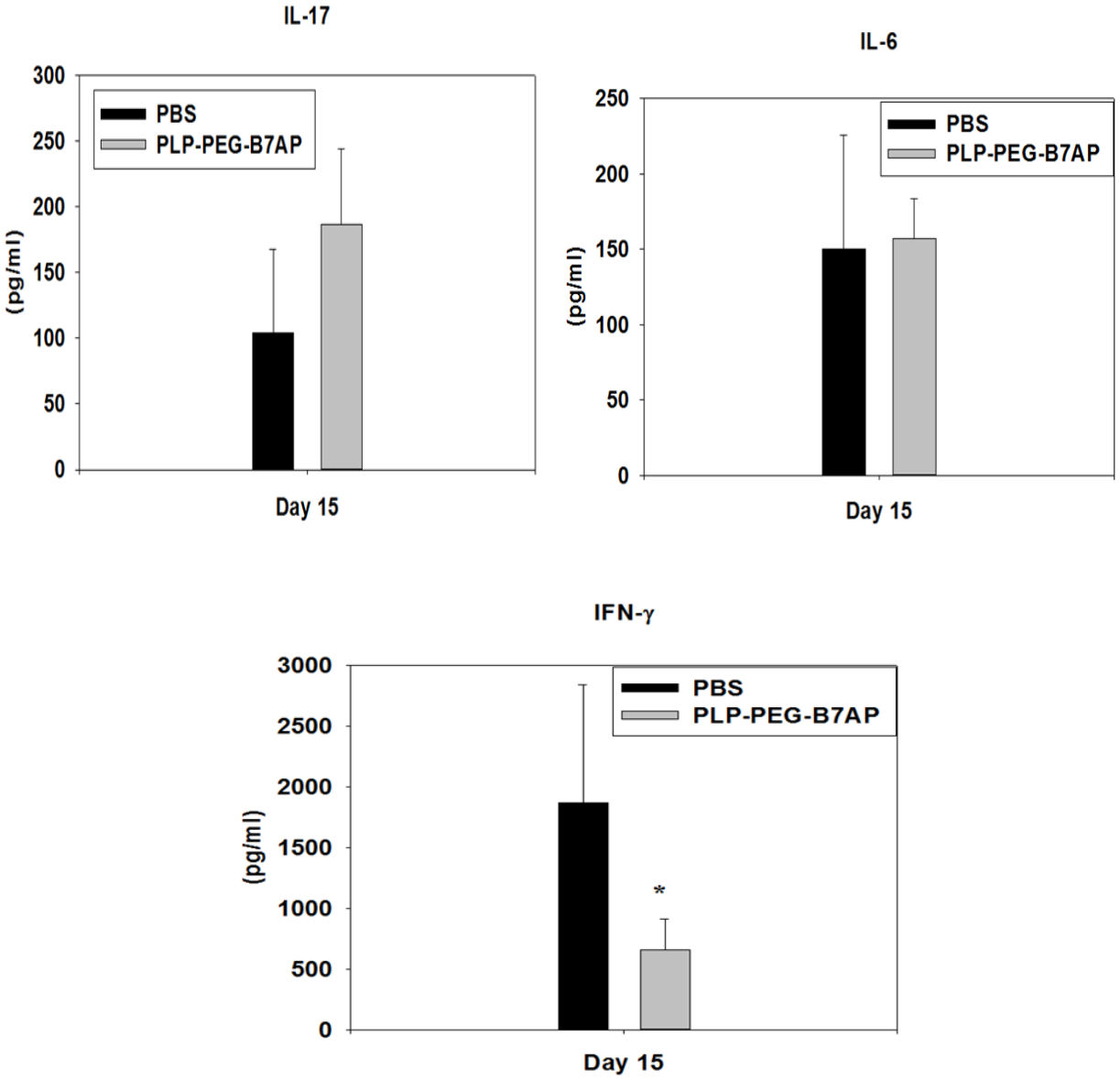

Figure 3.4. Day15 Cytokine Inflammatory Cytokine Analysis. Concentrations of pro-inflammatory cytokines (IFN-γ, IL-17, and IL-6) in cell culture supernatants from mice sacrificed on day 15. Splenocytes were isolated from the spleens of EAE mice treated with either PBS or PLP-PEG-B7AP on days –11, –8, and –5. The pooled splenocytes (n = 3) were stimulated in vitro with $PLP_{139-151}$, and the supernatants were isolated 72 h later for cytokine analysis. (p<0.001) * indicates significant difference.

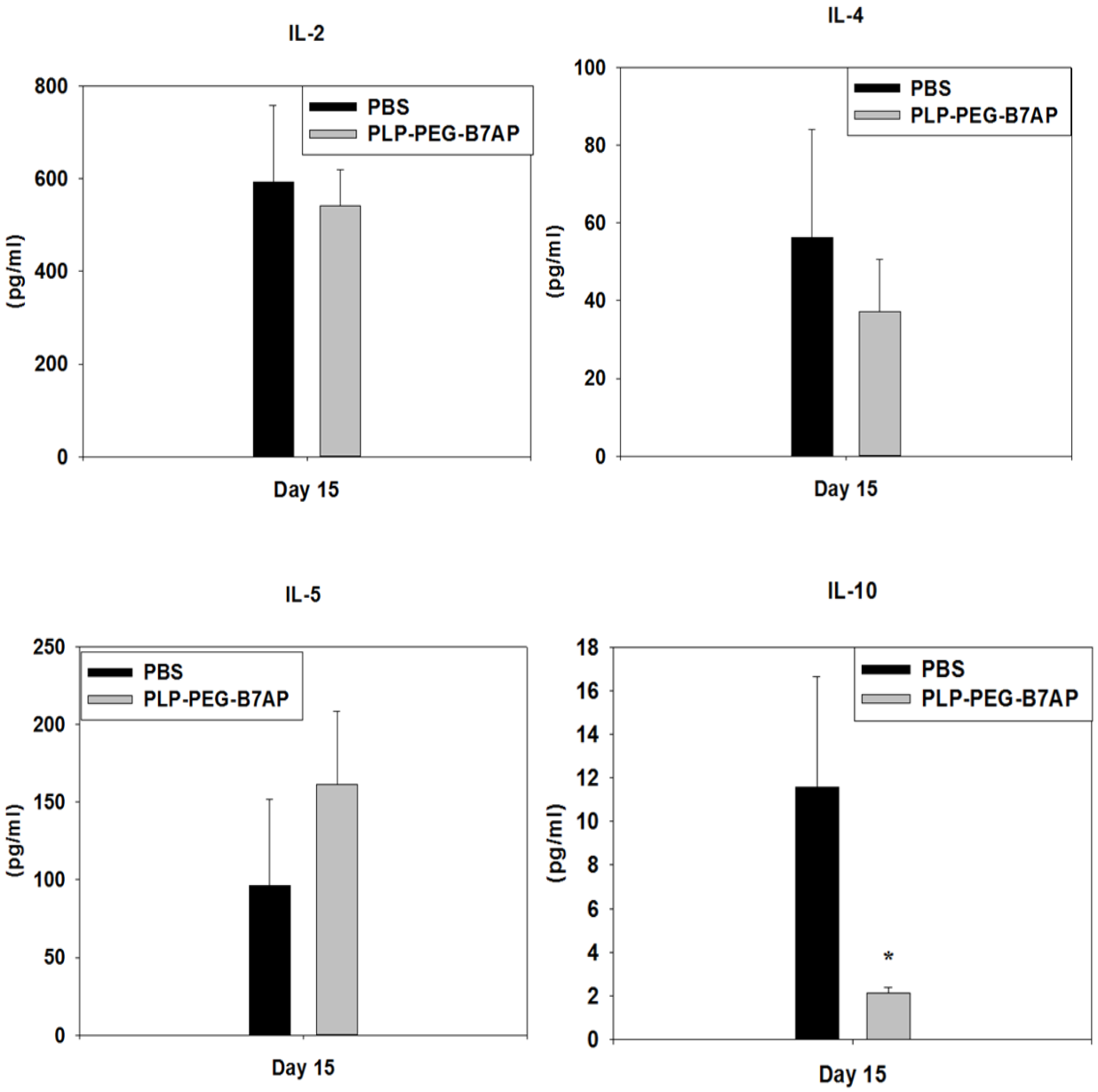

Figure 3.5. Day 15 regulatory cytokine analysis. Concentrations of regulatory/suppressor cytokines (IL-2, IL-4, IL-5, and IL-10) from the cell culture supernatants of splenocytes on day 15. Splenocytes were isolated from the spleens of EAE mice treated with either PBS or PLP-PEG-B7AP on days –11, –8, and –5. The pooled splenocytes (n = 3) were stimulated in vitro with $PLP_{139-151}$, and supernatants were isolated 72 h later for cytokine analysis. (p<0.001) * indicates significant difference.

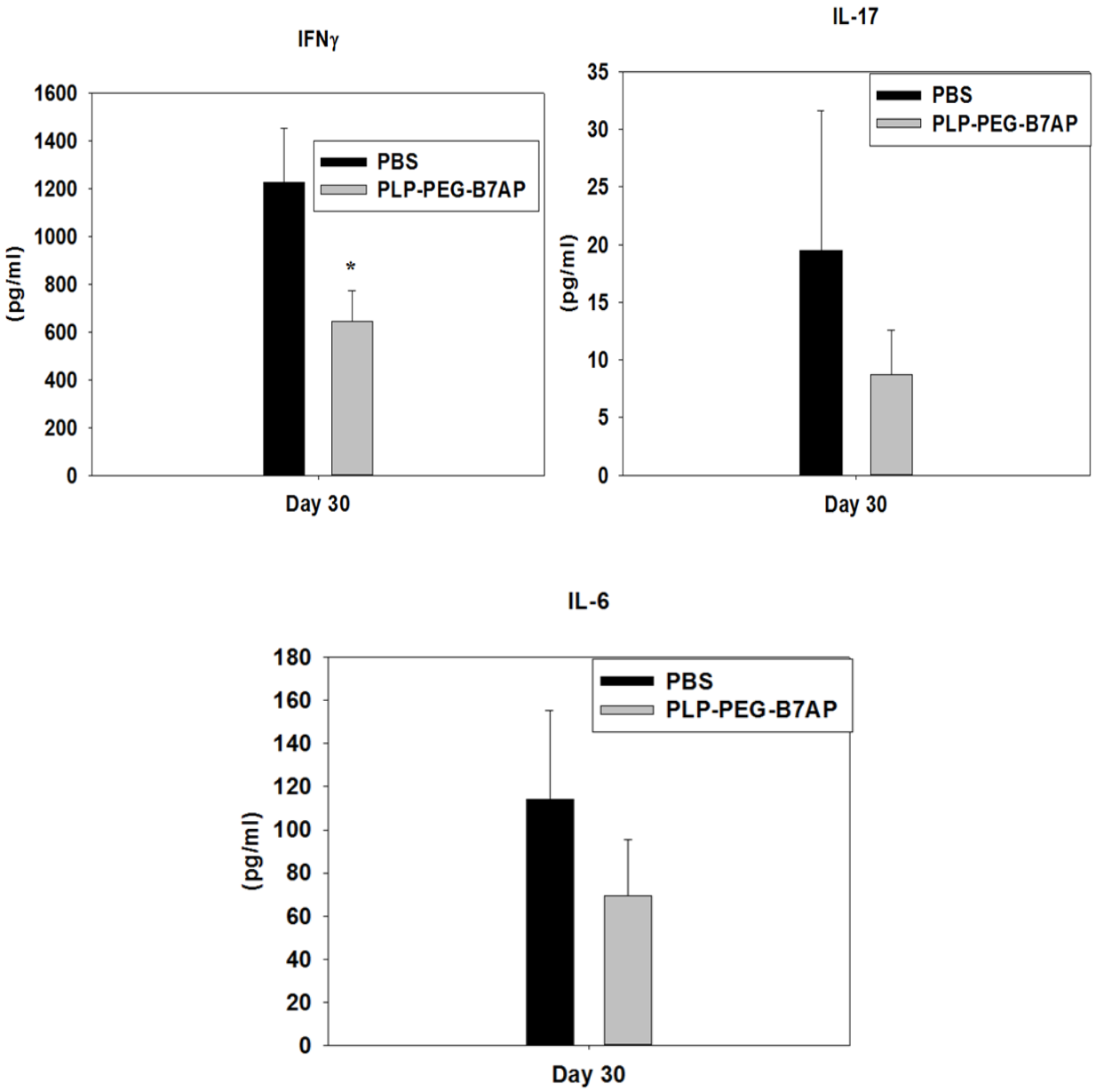

Figure 3.6. Day 30 inflammatory cytokine analysis. Concentrations of pro-inflammatory cytokines (IFN-γ, IL-17, and IL-6) in cell culture supernatants from mice sacrificed on day 30. Splenocytes were isolated from the spleens of EAE mice treated with either PBS or PLP-PEG-B7AP on days –11, –8, and –5. The pooled splenocytes (n = 3) were stimulated in vitro with $PLP_{139-151}$, and the supernatants were isolated 72 h later for cytokine analysis. (p<0.001) * indicates significant difference.

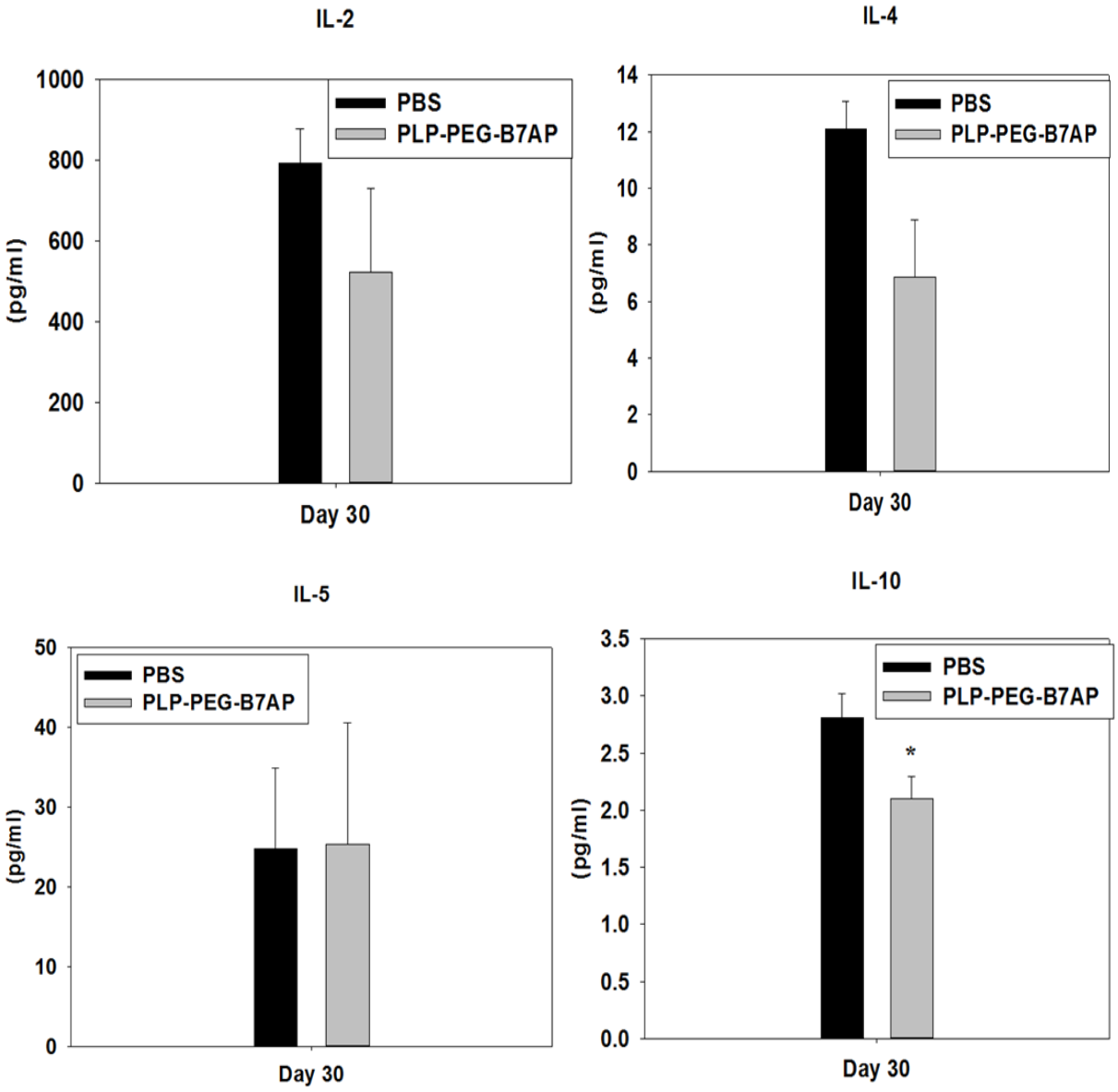

Figure 3.7. Day 30 regulatory cytokine analysis. Concentrations of regulatory/suppressor cytokines (IL-2, IL-4, IL-5, and IL-10) from the cell culture supernatants of splenocytes on day 30. Splenocytes were isolated from the spleens of EAE mice treated with either PBS or PLP-PEG-B7AP on days –11, –8, and –5. The pooled splenocytes (n = 3) were stimulated in vitro with $PLP_{139-151}$, and supernatants were isolated 72 h later for cytokine analysis. (p<0.001) * indicates significant difference.

3.4. Discussion

Peptide-based treatments for EAE have been used by Ishioka *et al.* to suppress EAE in mice [26]. Peptide antagonists of T-cell receptors (TCR) have been shown to significantly suppress and inactivate autoreactive T cells in EAE, presumably by blocking the signal-1 connection of MHC-II complex with the TCR. Although it is antigenic-specific, such a therapy may not be very efficient because it involves only one of the two important signals of T-cell activation. In an effort to create a more specific and efficent immuno-suppressive therapy, our group has developed bifunctional peptide inhibitor (BPI) molecules that have been shown to effectively suppress EAE [27, 28], type-1 diabetes (T1D) [29], and rheumatoid arthritis (RA). BPI treatments have been shown to be consistently more effective the corresponding treatment with parent antigenic peptide alone. This is due to the fact that BPI modulates both signal-1 and signal-2 during T-cell activation while the parent antigenic peptide modulates only signal-1 during the formation of the immunological synapse at the interface between T cells and APC. The proposed mechanism of action of BPI molecules is that it can simultaneously modulate both signal-1 (MHC-II/TCR) and signal-2 (ICAM-1/LFA-1 or CD28/B7), leading to specific suppression of EAE [2]. Previously, the BPI molecule PLP-B7AP showed significant suppression of disease in EAE mice when treated on days 4, 7, and 10 after induction of disease [Unpublished data].

In this study, the efficacy of PLP-PEG-B7AP to suppress EAE in "vaccine-like" injections was evaluated by administering the molecule on days 11, 8, and 5 before induction of the disease on day 0. Disease scores, incidence of disease, and changes in body weight were monitored from day 0 to day 30. A clear difference in disease scores can be observed in PLP-PEG-B7AP- and PLP-BPI-treated groups compared to the negative control group (PBS) (Figure 3.1). The PLP-

PEG-B7AP-treated group showed the lowest disease scores compared to other treated groups. This difference also correlates with the incidence of disease in treated mice (Figure 3.3). Half of the mice treated with PLP-PEG-B7AP were considered to be without disease incidence with disease scores of less than one while all of the PBS-treated mice developed disease scores of 1 or higher. It was difficult to compare the body weights between PBS- and PLP-PEG-B7AP-treated mice for the entire study (Figure 3.2). This is due to the lack of a sufficient number of PBS-treated animals for body weight measurements because some mice in the PBS-treated group developed very severe disease and had to be euthanized. This can explain why there is little difference in changes in body weight of mice between control and PLP and PLP-BPI groups on days 11, 12, and 13, when the disease was very severe. In other words, the body weights from animals with severe disease are not represented. However a clear difference in change in body weight can be observed between PBS and PLP-PEG-B7AP treated mice.

Splenocytes were also isolated and analyzed for production of cytokines to elucidate the type of T cells were generated during the disease on day 15 and day 30. Their seems to be no large differences in generation of regulatory and suppressor cytokines in PBS and PLP-PEG-B7AP groups, except in the production of IL-10 (Figure 3.4.). This suggests a limited effect of PLP-PEG-B7AP on the generation of regulatory and suppressor cytokines in the first appearance of disease on day 15. Also on day 15, inflammatory cytokines are at or near the same levels in PBS and PLP-PEG-B7AP treated groups, with the exception of IFN-γ (Figure 3.5.). IFN-γ is produced at far lower levels in PLP-PEG-B7AP treated mice than PBS. This suggest that PLP-PEG-B7AP is suppressing production of IFN-γ in the first appearance of disease on day 15.

Contrastingly on day 30 all inflammatory cytokines tested (IL-17, IL-6, and IFN-γ) were produced at higher levels in PBS-treated groups than in PLP-PEG-B7AP-treated groups (figure

3.6.). This suggests that PLP-PEG-B7AP can lower the proliferation of inflammatory T_H1 and T_H17 cells on day 30. Previously, treatment of EAE mice with PLP-B7AP on days 4, 7, and 10 also lowered the production of IL-17 observed on days 15 and 30; the production of IL-6 was lower on day 15 but not on day 30 in PLP-B7AP-treated compared to PBS-treated animals. Interestingly, production of IL-10, IL-2, and IL-4 on day 30 was at lower levels in PLP-PEG-B7AP-treated compared to PBS-treated groups while there was no change in IL-5 production (Figure 3.7.). In contrast, PLP-B7AP-treated mice (days 4, 7, and 10) compared to PBS-treated mice had higher production of IL-4 and IL-2 on days 15 and 30 and a higher production of IL-5 on day 30 but not day 15. The difference in cytokine production in PLP-B7AP- and PLP-PEG-B7AP-treated mice could be due to two reasons: (1) the linkers in PLP-PEG-B7AP and PLP-B7AP are different and (2) PLP-PEG-B7AP was injected as a "vaccine-like" administration while PLP-B7AP was administered as a prophylactic treatment. In the future, it will be necessary to perform side-by-side comparison of the efficacy and mechanisms of action of PLP-B7AP and PLP-PEG-B7AP.

To get an idea about the types of cells involved in demyelination of the CNS, cell staining of brains from PBS- and PLP-PEG-B7AP-treated mice was evaluated. Brain samples were taken on day 15 and 30 after induction of disease, which is the time period of the first occurrence and remission of disease, respectively. No difference in demyelination and lesion appearance or leukocyte infiltration was apparent [data not shown]. It is possible that on day 30 the animals were still in remission; typically, the disease relapse with high severity is after day 35. Perhaps it would be better to observe leukocyte infiltration to the brain during the relapse stage. Furthermore, infiltration of T cells would be better observed in the spinal cord than in the brain. It has been shown by Cross *et al*. that myelin reactive T cells infiltrate the spinal cord before

permeating the brain [30]. In the future, we will evaluate the infiltration of T cells into the spinal cord instead of the brain in both PLP-PEG-B7AP-treated and PBS-treated groups.

In conclusion, PLP-PEG-B7AP has been shown to effectively suppress EAE when delivered in a "vaccine-like" manner compared to PLP-BPI, PLP, and PBS. PLP-PEG-B7AP suppresses the production of inflammatory cytokines IL-17 and IFN-γ, suggesting that it also suppresses the proliferation of inflammatory T_H17 and T_H1 cells. Further studies will need to be done to understand the mechanism of the PLP-PEG-B7AP molecule and its effect on T-cell trafficking into the CNS and subsequent demyelination.

3.5. References

1. Fletcher, J.M., et al., *T cells in multiple sclerosis and experimental autoimmune encephalomyelitis.* Clinical and experimental immunology, 2010. **162**(1): p. 1-11.
2. Badawi, A.H. and T.J. Siahaan, *Immune modulating peptides for the treatment and suppression of multiple sclerosis.* Clinical immunology, 2012. **144**(2): p. 127–38.
3. Schmidt, S., *Candidate autoantigens in multiple sclerosis.* Multiple sclerosis, 1999. **5**(3): p. 147-60.
4. Bromley, S.K., et al., *The immunological synapse.* Annu Rev Immunol, 2001. **19**: p. 375-96.
5. Grakoui, A., et al., *The immunological synapse: a molecular machine controlling T cell activation.* Science, 1999. **285**(5425): p. 221-7.
6. Srinivasan, M., et al., *Suppression of experimental autoimmune encephalomyelitis using peptide mimics of CD28.* Journal of Immunology, 2002. **169**(4): p. 2180-2188.
7. McCoy, K.D. and G. Le Gros, *The role of CTLA-4 in the regulation of T cell immune responses.* Immunol Cell Biol, 1999. **77**(1): p. 1-10.
8. Truneh, A., et al., *Differential recognition by CD28 of its cognate counter receptors CD80 (B7.1) and B70 (B7.2): analysis by site directed mutagenesis.* Mol Immunol, 1996. **33**(3): p. 321-34.
9. Peach, R.J., et al., *Complementarity determining region 1 (CDR1)- and CDR3-analogous regions in CTLA-4 and CD28 determine the binding to B7-1.* J Exp Med, 1994. **180**(6): p. 2049-58.
10. Chen, J., et al., *Allogenic donor splenocytes pretreated with antisense peptide against B7 prolong cardiac allograft survival.* Clinical and experimental immunology, 2004. **138**(2): p. 245-50.
11. Lenschow, D.J., et al., *Differential effects of anti-B7-1 and anti-B7-2 monoclonal antibody treatment on the development of diabetes in the nonobese diabetic mouse.* J Exp Med, 1995. **181**(3): p. 1145-55.
12. Lenschow, D.J., T.L. Walunas, and J.A. Bluestone, *CD28/B7 system of T cell costimulation.* Annu Rev Immunol, 1996. **14**: p. 233-58.
13. Carreno, B.M. and M. Collins, *The B7 family of ligands and its receptors: new pathways for costimulation and inhibition of immune responses.* Annu Rev Immunol, 2002. **20**: p. 29-53.
14. Bajorath, J., W.J. Metzler, and P.S. Linsley, *Molecular modeling of CD28 and three-dimensional analysis of residue conservation in the CD28/CD152 family.* J Mol Graph Model, 1997. **15**(2): p. 135-9, 108-11.
15. Bar-Or, A., et al., *Molecular pathogenesis of multiple sclerosis.* Journal of neuroimmunology, 1999. **100**(1-2): p. 252-9.
16. Adorini, L., *Immunotherapeutic approaches in multiple sclerosis.* J Neurol Sci, 2004. **223**(1): p. 13-24.
17. Ridwan, R., et al., *Antigen-specific suppression of experimental autoimmune encephalomyelitis by a novel bifunctional peptide inhibitor: structure optimization and pharmacokinetics.* The Journal of pharmacology and experimental therapeutics, 2010. **332**(3): p. 1136-45.

18. Manikwar, P., et al., *Antigen-specific blocking of CD4-specific immunological synapse formation using BPI and current therapies for autoimmune diseases.* Medicinal research reviews, 2012. **32**(4): p. 727–64.
19. Wraith, D.C., *Therapeutic peptide vaccines for treatment of autoimmune diseases.* Immunology letters, 2009. **122**(2): p. 134-6.
20. Liblau, R.S., S.M. Singer, and H.O. McDevitt, *Th1 and Th2 CD4+ T cells in the pathogenesis of organ-specific autoimmune diseases.* Immunol Today, 1995. **16**(1): p. 34-8.
21. Minagar, A. and J.S. Alexander, *Blood-brain barrier disruption in multiple sclerosis.* Multiple sclerosis, 2003. **9**(6): p. 540-9.
22. Marelli-Berg, F.M., K. Okkenhaug, and V. Mirenda, *A two-signal model for T cell trafficking.* Trends Immunol, 2007. **28**(6): p. 267-73.
23. Rausch, M., et al., *MRI-based monitoring of inflammation and tissue damage in acute and chronic relapsing EAE.* Magn Reson Med, 2003. **50**(2): p. 309-14.
24. Badawi, A.H., et al., *Suppression of EAE and prevention of blood-brain barrier breakdown after vaccination with novel bifunctional peptide inhibitor.* Neuropharmacology, 2012. **62**(4): p. 1874-81.
25. Zhao, H., et al., *Immune response to controlled release of immunomodulating peptides in a murine experimental autoimmune encephalomyelitis (EAE) model.* Journal of controlled release : official journal of the Controlled Release Society, 2010. **141**(2): p. 145-52.
26. Franco, A., et al., *T cell receptor antagonist peptides are highly effective inhibitors of experimental allergic encephalomyelitis.* Eur J Immunol, 1994. **24**(4): p. 940-6.
27. Manikwar, P., et al., *I-domain-antigen conjugate (IDAC) for delivering antigenic peptides to APC: synthesis, characterization, and in vivo EAE suppression.* Bioconjugate chemistry, 2012. **23**(3): p. 509-17.
28. Kobayashi, N., et al., *Antigen-specific suppression of experimental autoimmune encephalomyelitis by a novel bifunctional peptide inhibitor.* The Journal of pharmacology and experimental therapeutics, 2007. **322**(2): p. 879-86.
29. Murray, J.S., et al., *Suppression of type 1 diabetes in NOD mice by bifunctional peptide inhibitor: modulation of the immunological synapse formation.* Chemical biology & drug design, 2007. **70**(3): p. 227-36.
30. Cross, A.H., T. O'Mara, and C.S. Raine, *Chronologic localization of myelin-reactive cells in the lesions of relapsing EAE: implications for the study of multiple sclerosis.* Neurology, 1993. **43**(5): p. 1028-33.

Conclusion and Future Directions

In this study, the novel MOG-PEG-IDAC molecule was successfully synthesized and characterized. Although the conjugation reaction to make the MOG-PEG-IDAC molecule is still inefficient, the yield of the reaction is better than that of MOG-IDAC. Because MOG-PEG-IDAC can be sufficiently produced, its efficacy is currently being evaluated. Future plans include: (a) evaluating different conditions for the conjugation reaction to improve the yield of MOG-PEG-IDAC, (b) determining the efficacy of MOG-PEG-IDAC as a vaccine-like treatment, (c) conjugating both MOG and PLP peptides simultaneously to the I-domain to produce PLP-MOG-IDAC, and (d) determining the efficacy of PLP-MOG-IDAC in PLP- and MOG-stimulated EAE.

PLP-PEG-B7AP was found to be effective in suppressing EAE as vaccine-like treatment. This molecule suppresses inflammatory cytokine production from isolated splenocytes compared to those from PBS-treated mice. However, lower levels of regulatory/suppressor cytokines (i.e., IL-10, IL-4) were found in PLP-PEG-B7AP-treated mice compared to PBS-treated mice during first appearance of disease day 15 and remission on day 30. This is in contrast to PLP-B7AP-treated animals, which showed higher levels of regulatory cytokines compared to PBS-treated animals. The difference between cytokines produced by PLP-PEG-B7AP and PLP-B7AP could be due to the vaccine-like administration of PLP-PEG-B7AP compared to prophylactic treatment with PLP-B7A. Secondly, the presence of PEG groups in PLP-PEG-B7AP may alter its mechanism of action compared to that of PLP-B7AP. Finally, further analysis of regulatory T cells will be carried out by detecting CTLA-4 and FOXp3 as marker molecules on T cells. Currently, there is an ongoing study to evaluate the effect of MOG-PEG-B7AP in suppressing MOG-stimulated EAE in mice. If suppression of EAE is demonstrated, multiantigen BPI (i.e.,

MOG-PLP-B7AP) with a B7AP peptide connected to the MOG and PLP peptides will be synthesized and evaluated for suppressing MOG- and PLP-stimulated EAE. This may allow the MOG-PLP-B7AP to prevent antigenic spreading in MS in the future.